Coronado Systems

Robust Industrial Control

Course Notes

Part 2: Robust and Optimal Control

REV. 0 , JULY 2000

1 Norms of signals and systems

Norms of signals and systems are used to quantify the performance and robustness of a control system. They are used in robust optimal control theory.

1.1 Vector and matrix norms

In finite-dimensional vector spaces, it is convenient to define norms to measure the length of vectors, and matrix norms to measure the maximum "gain" of the matrix.

The 2-norm (or Euclidean norm) of an n-dimensional complex vector $x \in \mathbb{C}^n$ is defined as:

$$\begin{aligned} \|x\|_2 &= \left(x^* x\right)^{\frac{1}{2}} \\ &= \left(|x_1|^2 + |x_2|^2 + \cdots + |x_n|^2\right)^{\frac{1}{2}} \end{aligned} \tag{0.1}$$

where x^* denotes the conjugate transpose of x. The *spectral norm* of an $n \times m$ complex matrix $Q \in \mathbb{C}^{n \times m}$ is defined as its maximum singular value $\sigma_{\max}$:

$$\|Q\| = \sigma_{\max}(Q) = \left[\lambda_{\max}\left(Q^* Q\right)\right]^{\frac{1}{2}}, \tag{0.2}$$

where $\lambda_{\max}$ denotes the maximum eigenvalue. This matrix norm represents the maximum input-output gain in terms of 2-norms of input and output vectors. One can show that, with $x \in \mathbb{R}^m$:

$$\|Q\| = \max_{x \neq 0} \frac{\|Qx\|_2}{\|x\|_2} = \max_{\|x\|_2 \leq 1} \|Qx\|_2 = \max_{\|x\|_2 = 1} \|Qx\|_2 \tag{0.3}$$

Example

Consider the complex linear matrix equation $y = Qx$ where

$$Q = \begin{bmatrix} \frac{1}{2} + j\frac{\sqrt{3}}{2} & -1 \\ 1 & 2 \end{bmatrix}. \tag{0.4}$$

The spectral norm of the matrix is given by:

$$\|Q\| = \sigma_{\max}(Q) = \left[\lambda_{\max}\left(Q^{*}Q\right)\right]^{\frac{1}{2}}$$

$$= \left[\lambda_{\max}\left(\begin{bmatrix} \frac{1}{2} - j\frac{\sqrt{3}}{2} & 1 \\ -1 & 2 \end{bmatrix}\begin{bmatrix} \frac{1}{2} + j\frac{\sqrt{3}}{2} & -1 \\ 1 & 2 \end{bmatrix}\right)\right]^{\frac{1}{2}} \tag{0.5}$$

$$= \left[\lambda_{\max}\left(\begin{bmatrix} 2 & \frac{3}{2} + j\frac{\sqrt{3}}{2} \\ \frac{3}{2} - j\frac{\sqrt{3}}{2} & 5 \end{bmatrix}\right)\right]^{\frac{1}{2}} = \sqrt{5.79} = 2.41$$

Thus the maximum amplification from the 2-norm of the input vector to the 2-norm of the output vector will be a gain of 2.41. If we randomly select an input vector, say $x = \begin{bmatrix} 1+j \\ 3 \end{bmatrix}$ for which $\|x\|_2 = \left(\begin{bmatrix} 1-j & 3 \end{bmatrix}\begin{bmatrix} 1+j \\ 3 \end{bmatrix}\right)^{\frac{1}{2}} = \sqrt{2+9} = 3.317$, then the output vector is

$$y = \begin{bmatrix} \frac{1}{2} + j\frac{\sqrt{3}}{2} & -1 \\ 1 & 2 \end{bmatrix}\begin{bmatrix} 1+j \\ 3 \end{bmatrix} = \begin{bmatrix} -\frac{5+\sqrt{3}}{2} + j\frac{1+\sqrt{3}}{2} \\ 7+j \end{bmatrix} \tag{0.6}$$

and its 2-norm is computed to be $\|y\|_2 = 7.712$. The gain produced by the matrix is thus $\frac{\|y\|_2}{\|x\|_2} = \frac{7.712}{3.317} = 2.325$ which is smaller than its norm $\|Q\| = 2.41$ as expected.

1.2 L_2-norm for finite-energy signals

The $\mathcal{L}_2$-norm (or 2-norm) of a signal $x(t)$ is the square root of its total energy over -∞ < t < ∞ and is defined as:

$$\|x\|_2 = \left(\int_{-\infty}^{\infty} |x(t)|^2 \, dt\right)^{\frac{1}{2}} \tag{0.7}$$

The set of all finite-energy signals is called the space $\mathcal{L}_2$:

$$\mathcal{L}_2 := \left\{x : \|x\|_2 < +\infty\right\} \tag{0.8}$$

A "large" signal would have a large $\mathcal{L}_2$-norm, hence it is a measure of the size of a signal. In a servo system, the objective is to minimize the tracking error signal $e(t) = y_d(t) - y(t)$. It makes sense to try to minimize its $\mathcal{L}_2$-norm $\|e\|_2$ if the reference signal $y_d(t)$ belongs to $\mathcal{L}_2$.

The following result allows us to compute the $\mathcal{L}_2$-norm in the frequency domain using the Fourier transform $\hat{x}(j\omega)$ of the signal.

<u>Parseval's Theorem</u>

$$\|x\|_2^2 = \int_{-\infty}^{\infty} \|x(t)\|^2 \, dt = \frac{1}{2\pi} \int_{-\infty}^{\infty} \|\hat{x}(j\omega)\|^2 \, d\omega . \tag{0.9}$$

1.3 Power "norm" for finite-power signals

The power "norm" of a signal $x(t)$ is the square root of its total average power over -∞ < t < ∞ and is defined as:

$$pow(x) := \left(\lim_{T \to +\infty} \frac{1}{2T} \int_{-T}^{T} |\, x(t) \,|^2 \, dt \right)^{\frac{1}{2}} . \tag{0.10}$$

Note that for periodic signals, it is sufficient to compute the average power over one period only:

$$pow(x) := \left(\frac{1}{T} \int_{0}^{T} |\, x(t) \,|^2 \, dt, \right)^{\frac{1}{2}} \; x \text{ periodic of period } T . \tag{0.11}$$

Strictly speaking, the function $pow(x)$ is not a norm because it can be equal to 0 for nonzero signals, e.g., for signals in $\mathcal{L}_2$. Apart from that, it behaves like a regular norm. For instance, the triangle inequality holds:

$$pow(x + y) \le pow(x) + pow(y) . \tag{0.12}$$

The set $\mathcal{P}$ of all finite-power signals is defined as follows:

$$\mathcal{P} := \{ x : pow(x) < +\infty \} \tag{0.13}$$

Examples: $x(t) = 4$ has infinite energy but a power norm of 4 (and a power of 16):

$$pow(x) = \left(\lim_{T \to \infty} \frac{1}{2T} \int_{-T}^{T} 4^2 \, dt \right)^{\frac{1}{2}} = \left(\lim_{T \to \infty} \frac{4^2}{2T} 2T \right)^{\frac{1}{2}} = 4 . \tag{0.14}$$

For a periodic complex exponential $x(t) = Ce^{j\omega t}$ of period $T = \dfrac{2\pi}{\omega}$:

$$pow(x) = \left(\frac{1}{T} \int_0^T | Ce^{j\omega t} |^2 \, dt \right)^{\frac{1}{2}} = \left(\frac{| C |^2}{T} \int_0^T dt \right)^{\frac{1}{2}} = | C | \tag{0.15}$$

Note that $e^{j\omega_0 t}$ has total average power and power norm equal to 1.

1.4 L_2 norm of LTI systems and the space H_2 of stable causal systems

We consider the class of LTI causal systems. The input-output equation for such systems has the form of a convolution:

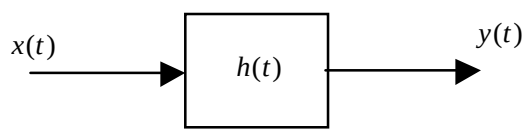

$$y(t) = \int_{-\infty}^{+\infty} x(\tau) h(t-\tau) d\tau \tag{0.16}$$

where $h(t)$ is the impulse response of the system. For MIMO systems, $h(t)$ is a matrix function. The transfer function of the system is given by

$$H(s) = \int_{-\infty}^{+\infty} h(t) e^{-st} dt \tag{0.17}$$

and its frequency response is simply $H(s)\big|_{s=j\omega} = H(j\omega)$. Recall that in the Laplace domain and in the frequency domain, we have much simpler input-output relationships given by:

$$\hat{y}(s) = H(s)\hat{x}(s) \,. \tag{0.18}$$

$$\hat{y}(j\omega) = H(j\omega)\hat{x}(j\omega) \,. \tag{0.19}$$

We will consider finite-dimensional differential LTI systems so that their transfer functions are rational. We say that $H(s)$ is: *proper* if $H(j\infty)$ is finite, *strictly proper* if $H(j\infty) = 0$, and *biproper* if $H(s)$ and $H^{-1}(s)$ are both proper (i.e., if $0 < H(j\infty) < \infty$). Also recall that $H(s)$ is BIBO stable iff all of its poles are in the open left half-plane *and* it is proper.

The $\mathcal{L}_2$-norm (or 2-norm) of a system is defined as:

$$\|H\|_2 = \left(\frac{1}{2\pi} \int_{-\infty}^{\infty} trace\left\{ H(j\omega)^* H(j\omega) \right\} d\omega \right)^{\frac{1}{2}} \tag{0.20}$$

The set of all systems with finite $\mathcal{L}_2$-norm is called $\mathcal{L}_2$: mathematically it is the same space as defined by (0.8). Parseval's theorem gives us a way to compute the $\mathcal{L}_2$-norm in the time domain from the impulse response matrix:

$$\|H\|_2 = \left(\frac{1}{2\pi} \int_{-\infty}^{\infty} trace\left\{ H^*(j\omega) H(j\omega) \right\} d\omega \right)^{\frac{1}{2}} = \left(\int_{-\infty}^{\infty} trace\left\{ h^*(t) h(t) \right\} dt \right)^{\frac{1}{2}}. \tag{0.21}$$

If $H(s)$ causal, then

$$\|H\|_2 = \left(\frac{1}{2\pi} \int_{-\infty}^{\infty} trace\left\{ H^*(j\omega) H(j\omega) \right\} d\omega \right)^{\frac{1}{2}} = \left(\int_{0}^{\infty} trace\left\{ h^*(t) h(t) \right\} dt \right)^{\frac{1}{2}}. \tag{0.22}$$

The space $\mathcal{H}_2$ is the space of all stable, causal systems with finite $\mathcal{L}_2$-norm:

$$\mathcal{H}_2 := \left\{ H \text{ causal, stable } : \|H\|_2 < +\infty \right\}. \tag{0.23}$$

Another way to define $\mathcal{H}_2$ is to say that it is the subspace of systems in $\mathcal{L}_2$ that are analytic in the closed RHP. The orthogonal complement of $\mathcal{H}_2$ is denoted as $\mathcal{H}_2^{\perp}$. It consists of systems in $\mathcal{L}_2$ that are analytic in the closed LHP, so that $\mathcal{L}_2 = \mathcal{H}_2 \oplus \mathcal{H}_2^{\perp}$. The systems in $\mathcal{H}_2^{\perp}$ are actually anticausal ($h(t) = 0,\ t < 0$), stable systems with finite $\mathcal{L}_2$-norm.

Orthogonality of the system spaces $\mathcal{H}_2$ and $\mathcal{H}_2^{\perp}$ means that any system $H(s)$ in $\mathcal{L}_2$ can be decomposed as a sum of its $\mathcal{H}_2$ component and its $\mathcal{H}_2^{\perp}$ component as follows:

$$H(s) = \left\{ H(s) \right\}_{\mathcal{H}_2} + \left\{ H(s) \right\}_{\mathcal{H}_2^{\perp}}, \tag{0.24}$$

where $\left\{ H(s) \right\}_{\mathcal{H}_2}$ means taking the stable terms (with LHP poles) in the partial fraction expansion of $H(s)$, and $\left\{ H(s) \right\}_{\mathcal{H}_2^{\perp}}$ means taking the unstable terms (with RHP poles) in the partial fraction expansion.

The most important consequence of orthogonality is the following:

$$\|H\|_2^2 = \left\|\{H\}_{\mathcal{H}_2^\perp}\right\|_2^2 + \left\|\{H\}_{\mathcal{H}_2}\right\|_2^2. \tag{0.25}$$

This comes from the definition of the inner product in $\mathcal{L}_2$, and orthogonality of $\mathcal{H}_2$ and $\mathcal{H}_2^\perp$ which comes from the fact that the product of the corresponding impulse response components corresponding to $\{H(s)\}_{\mathcal{H}_2^\perp}$ $h_0(t) = 0, t < 0$, and $\{H(s)\}_{\mathcal{H}_2}$ $h_\perp(t) = 0, t \geq 0$ is 0.

1.4.1 How to compute the $\mathcal{L}_2$-norm of stable systems

Suppose that $H(s)$ is stable and strictly proper (so that it has a finite $\mathcal{L}_2$-norm). Further assume that we have a state-space realization $(A, B, C, 0)$ of $H(s)$. Define the *controllability grammian* matrix:

$$L := \int_0^{+\infty} e^{At} BB^T e^{A^T t} dt\,. \tag{0.26}$$

It can be shown that L satisfies the *Lyapunov equation:*

$$AL + LA^T + BB^T = 0 \tag{0.27}$$

Then a formula to compute the $\mathcal{L}_2$-norm of the system (also called $\mathcal{H}_2$-norm since the system is stable and hence belongs to $\mathcal{H}_2$) is given by:

$$\|H\|_2 = \left[trace\left(CLC^T\right)\right]^{\frac{1}{2}}. \tag{0.28}$$

Thus, the procedure consists of computing the controllability grammian matrix L by solving the Lyapunov equation (0.27) (*lyap* command in Matlab) and then to compute $\|H\|_2$ using (0.28). The Matlab Mu-Analysis and Synthesis toolbox has the command *h2norm* that does all this.

1.5 L_∞ norm of LTI systems and the space H_∞ of stable systems

The $\mathcal{L}_\infty$-norm (or ∞-norm) of a system is defined as:

$$\|H\|_\infty = \sup_{\omega \in \mathbb{R}} |H(j\omega)| \tag{0.29}$$

It is the maximum gain of the frequency response of the system. The set of all systems with finite $\mathcal{L}_\infty$-norms is called $\mathcal{L}_\infty$ and is defined by

$$\mathcal{L}_\infty := \left\{H : \|H\|_\infty < +\infty\right\}. \tag{0.30}$$

The space $\mathcal{H}_\infty$ is the space of all causal, stable systems with finite $\mathcal{L}_\infty$ -norm:

$$\mathcal{H}_\infty := \left\{ H \text{ causal, stable } : \|H\|_\infty < +\infty \right\}. \tag{0.31}$$

1.5.1 How to compute the $\mathcal{L}_\infty$ -norm of stable systems

Suppose that $H(s)$ is stable and proper. Further assume that we have a state-space realization (A, B, C, D) of $H(s)$. Define the $2n \times 2n$ *Hamiltonian matrix*:

$$J := \begin{bmatrix} A & BB^T \\ -C^T C & -A^T \end{bmatrix}. \tag{0.32}$$

We have the following result telling us whether the $\mathcal{L}_\infty$ -norm of the system (also called $\mathcal{H}_\infty$ -norm since the system is stable and hence belongs to $\mathcal{H}_\infty$) is less than 1.

Theorem:

$\|H\|_\infty < 1$ if and only if J has no eigenvalues on the $j\omega$ -axis.

This result suggests a bisection search to find the $\mathcal{H}_\infty$ -norm of the transfer matrix: Try a large positive value γ_0 first to see if $\|H\|_\infty < \gamma_0$ which is equivalent to $\left\|\gamma_0^{-1} H\right\|_\infty < 1$. That is, check if

$$J(\gamma_0) := \begin{bmatrix} A & \gamma_0^{-2} BB^T \\ -C^T C & -A^T \end{bmatrix} \tag{0.33}$$

has no eigenvalues on the $j\omega$ -axis. If it doesn't, then select a new $\gamma_1 = \frac{1}{2}\gamma_0$ and check again if $J(\gamma_1)$ has no eigenvalues on the $j\omega$ -axis. If it doesn't, then reduce gamma by half again. if it does have eigenvalues on the $j\omega$ -axis, then select the middle value $\gamma_2 = \frac{1}{2}(\gamma_0 + \gamma_1)$, and continue the iteration until two consecutive values of gamma representing lower and upper bounds on $\|H\|_\infty$ are found to be close enough. The Matlab command *hinfnorm* uses this algorithm to compute $\|H\|_\infty$.

1.6 Relationships between input and output signal norms and system norms

We discussed the fact that the spectral norm of a matrix can be interpreted as its maximum gain from the norm of the input vector to the norm of the output vector. System norms can also be interpreted this way. Namely, the maximum gain of a system from the $\mathcal{L}_2$ -norm of its input signal $x(t)$ to the $\mathcal{L}_2$ -norm of its output signal $y(t)$ is given by the $\mathcal{H}_\infty$ -norm of its transfer matrix:

$$\|H\|_\infty = \sup_{x\neq 0}\frac{\|y\|_2}{\|x\|_2} = \max_{\|x\|_2\leq 1}\|H(j\omega)\hat{x}(j\omega)\|_2 = \max_{\|x\|_2=1}\|H(j\omega)\hat{x}(j\omega)\|_2 \qquad (0.34)$$

It turns out that the $\mathcal{H}_\infty$-norm is also the maximum power gain of the system:

$$\|H\|_\infty = \sup_{pow(x)\neq 0}\frac{pow(y)}{pow(x)} = \max_{pow(x)\leq 1} pow[H(j\omega)\hat{x}(j\omega)] = \max_{pow(x)=1} pow[H(j\omega)\hat{x}(j\omega)] \qquad (0.35)$$

For SISO systems, this means that the $\mathcal{H}_\infty$-norm, seen as the peak value of the magnitude of the Bode plot at some frequency ω_0, is the maximum amplification of a sinusoidal input (a power signal) at frequency ω_0.

The $\mathcal{H}_2$-norm of a system equals the $\mathcal{L}_2$-norm of the output $\|y\|_2$ for an impulse $\delta(t)$ at its input (or $\delta(t)U$ where U is an arbitrary complex unitary matrix, in the MIMO case).

2 H_2 Optimal Control

$\mathcal{H}_2$ optimal control is a theory to design finite-dimensional LTI controllers that minimize the $\mathcal{H}_2$-norm of the closed-loop system. But first we will study the algebraic Riccati equation which is ubiquitous in optimal control theory.

2.1 Algebraic Riccati Equations

Let A, Q, R be real $n\times n$ matrices with Q, R symmetric. Then an *algebraic Riccati equation* (ARE) is the following matrix equation:

$$A^*X + XA + XRX + Q = 0 \qquad (0.36)$$

Associated with this ARE is the $2n\times 2n$ *Hamiltonian matrix*:

$$H := \begin{bmatrix} A & R \\ -Q & -A^* \end{bmatrix} \qquad (0.37)$$

This matrix will be used to solve the ARE for the matrix X. Note that the ARE can be written as:

$$\begin{bmatrix} X & -I \end{bmatrix} H \begin{bmatrix} I \\ X \end{bmatrix} = \begin{bmatrix} X & -I \end{bmatrix}\begin{bmatrix} A & R \\ -Q & -A^* \end{bmatrix}\begin{bmatrix} I \\ X \end{bmatrix} = 0. \qquad (0.38)$$

The *Ric* function is now defined. Assume that Hamiltonian matrix H has no eigenvalue on the imaginary axis. Then, it must have n eigenvalues in the open right half-plane and n eigenvalues in

the open left half-plane. Consider the n-dimensional invariant spectral subspace $\mathcal{X}_-(H)$ corresponding to the n eigenvalues of H in the open left half-plane. By finding a basis for $\mathcal{X}_-(H)$, i.e., by putting the n eigenvectors corresponding to the eigenvalues in the open LHP into a matrix and partitioning, we get:

$$\mathcal{X}_-(H) = Ra\left\{\begin{bmatrix} X_1 \\ X_2 \end{bmatrix}\right\}, \quad X_1, X_2 \in \mathbb{C}^{n\times n} \tag{0.39}$$

If X_1 is nonsingular, then we can define $X := X_2 X_1^{-1}$ and the Hamiltonian matrix H uniquely defines X. Thus the relationship $H \mapsto X$ is a function, and this function is called Ric:

$$\mathrm{Ric}: \mathrm{dom}\{\mathrm{Ric}\} \subset \mathbb{R}^{2n\times 2n} \to \mathbb{R}^{n\times n} \tag{0.40}$$

The domain $\mathrm{dom}\{\mathrm{Ric}\}$ of the function Ric is taken to be Hamiltonian matrices that

(i) have no eigenvalues on the imaginary axis, and

(ii) have a nonsingular X_1.

The following result states that $X := X_2 X_1^{-1}$ is a solution to the algebraic Riccati equation:

Theorem: ARE

Suppose that $H \in \mathrm{dom}\{\mathrm{Ric}\}$*, and* $X = \mathrm{Ric}(H)$*. Then:*

(i) X *is real symmetric,*

(ii) X *satisfies the ARE,*

(iii) $A + RX$ *is stable (all of its eigenvalues are in the open LHP).*

We prove only (ii) as follows. From (0.38), the left-hand side of the ARE can be written as:

$$
\begin{aligned}
\begin{bmatrix} X & -I \end{bmatrix} H \begin{bmatrix} I \\ X \end{bmatrix} &= \begin{bmatrix} X & -I \end{bmatrix} H \begin{bmatrix} I \\ X \end{bmatrix} \\
&= \begin{bmatrix} X_2 X_1^{-1} & -I \end{bmatrix} H \begin{bmatrix} I \\ X_2 X_1^{-1} \end{bmatrix} \\
&= \begin{bmatrix} X_2 X_1^{-1} & -I \end{bmatrix} H \begin{bmatrix} X_1 \\ X_2 \end{bmatrix} X_1^{-1} \\
&= \begin{bmatrix} X_2 X_1^{-1} & -I \end{bmatrix} \begin{bmatrix} X_1 \\ X_2 \end{bmatrix} \begin{bmatrix} \lambda_1 & 0 & \cdots & 0 \\ 0 & \lambda_2 & & \vdots \\ \vdots & & \ddots & 0 \\ 0 & 0 & \cdots & \lambda_n \end{bmatrix} X_1^{-1} \\
&= 0
\end{aligned}
\tag{0.41}
$$

Suppose that the Hamiltonian matrix has the form:

$$
H = \begin{bmatrix} A & -BB^* \\ -C^*C & -A^* \end{bmatrix} \tag{0.42}
$$

Then it can be shown that $H \in \mathrm{dom}\{\mathrm{Ric}\}$ if the pair (A, B) is controllable and the pair (A, C) is observable.

2.2 Problem setup

Consider the general block diagram of a feedback control system shown below.

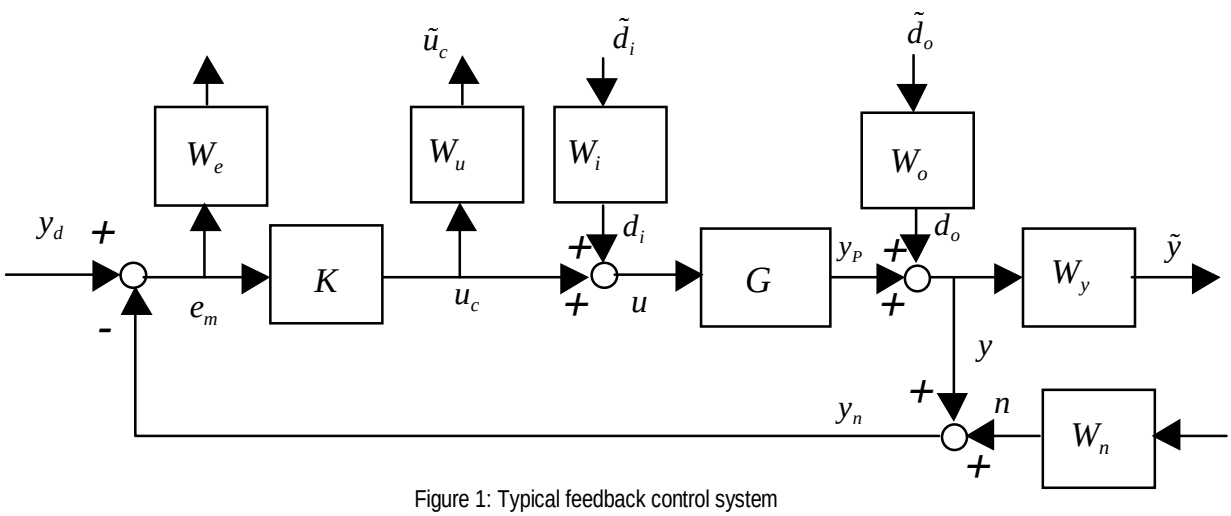

Figure 1: Typical feedback control system

The *weighting functions* W_x are added for different reasons (although they are rarely all present in a given design):

- To enforce closed-loop performance specs (weighting functions on output signals)
- To represent the frequency contents of disturbances and noises
- To normalize signals with different units in an optimal control setting

It is in fact essential that appropriate weighting functions be used in order to utilize the optimal control theory discussed in this section ($\mathcal{H}_2$) and in the next section ($\mathcal{H}_\infty$). So an important step in the controller design process is to select reasonable weighting functions W_d, W_e, W_y, W_u. This is not trivial. Many times, these weighting functions can be used as design parameters to achieve a good tradeoff between conflicting closed-loop objectives.

For simplicity, we assume that $\tilde{d}_i = 0, \tilde{n} = 0$, and we consider the regulator problem where the effect of the output disturbance $\tilde{d}_o$ on the weighted output $\tilde{y}$ must be minimized. This system can be recast as a linear fractional transformation (LFT) as follows.

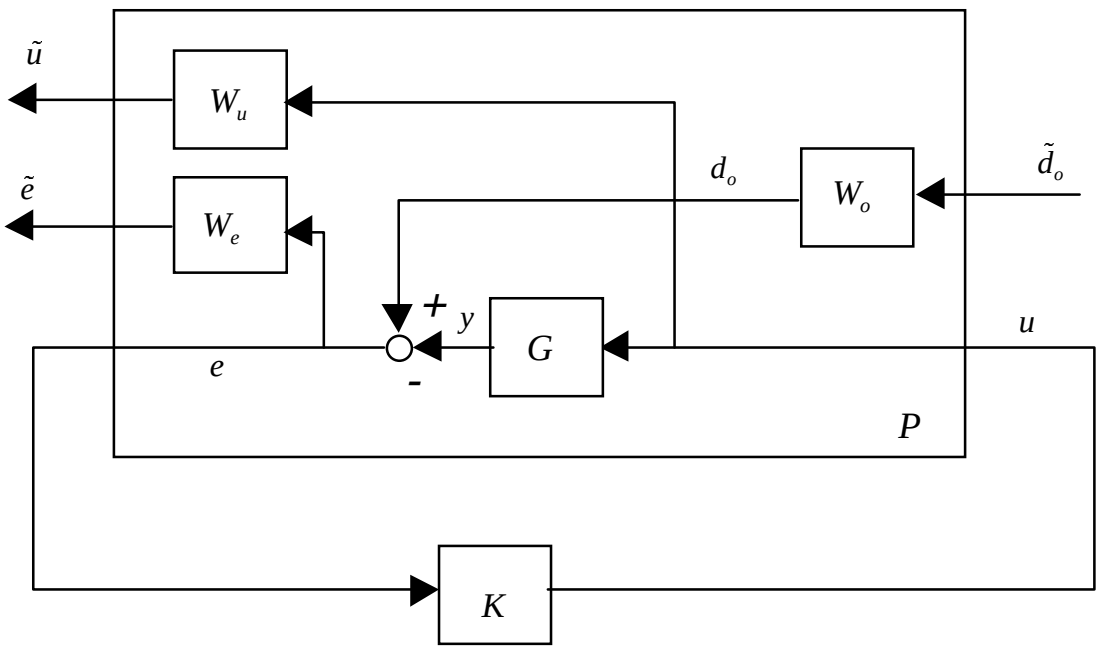

Figure 2: Typical setup for $\mathcal{H}_2$-optimal control design

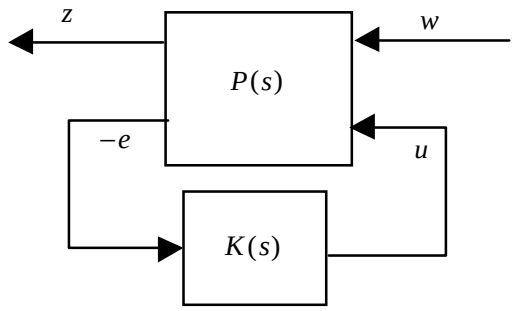

Figure 3: Standard LFT diagram for $\mathcal{H}_2$-optimal control design

Where $P(s) := \begin{bmatrix} P_{11}(s) & P_{12}(s) \\ P_{21}(s) & P_{22}(s) \end{bmatrix}$, and the transfer matrix entries of this *generalized plant* are readily obtained from the paths relating each input signal to each output signal. Here we have:

$$\begin{aligned} P_{11}(s) &= 0 \\ P_{12}(s) &= \begin{bmatrix} W_u \\ W_e G \end{bmatrix} \\ P_{21}(s) &= W_o \\ P_{22}(s) &= -G \end{aligned} \tag{0.43}$$

The weighting function $W_u(s)$ can be used to constrain the control signal while $W_e(s)$ can be used to reduce the sensitivity at low frequencies. Weighting function $W_o(s)$ can be used to model the power spectral density or energy-density spectrum of the output disturbance. Once the control system is put in the form of the so-called standard $\mathcal{H}_2$ problem (in LFT form), the minimization problem becomes:

$$\min_{K \in \mathcal{S}} \left\| T_{zw} \right\|_2 \tag{0.44}$$

where

$$T_{zw}(s) = \mathcal{F}_L\left[P(s), K(s)\right] = P_{11}(s) + P_{12}(s)K(s)\left[I - P_{22}(s)K(s)\right]^{-1} P_{21}(s) \tag{0.45}$$

is the closed-loop transfer matrix from the exogenous input w to the output z. One can then use the following result on $\mathcal{H}_2$ optimal control (very similar to LQG): Suppose that a state-space realization of $P(s)$ is given by

$$P(s) = \left[\begin{array}{c|cc} A & B_1 & B_2 \\ \hline C_1 & 0 & D_{12} \\ C_2 & D_{21} & 0 \end{array}\right] \tag{0.46}$$

Notice the special off-diagonal structure of D: D_{22} is assumed to be 0 so that $P_{22}(s)$ is strictly proper, and D_{11} is assumed to be 0 so that $P_{11}(s)$ is also strictly proper (which is a necessary condition for $P_{11}(s)$ to be in $\mathcal{H}_2$.)

First define $R_1 = D_{12}^* D_{12}$ and $R_2 = D_{21}^* D_{21}$, and the two Hamiltonian matrices:

$$H_2 := \begin{bmatrix} A - B_2 R_1^{-1} D_{12}^* C_1 & -B_2 R_1^{-1} B_2^* \\ -C_1^* \left(I - D_{12} R_1^{-1} D_{12}^*\right) C_1 & -\left(A - B_2 R_1^{-1} D_{12}^* C_1\right)^* \end{bmatrix} \tag{0.47}$$

$$J_2 := \begin{bmatrix} \left(A - B_1 D_{21}^* R_2^{-1} C_2\right)^* & -C_2^* R_2^{-1} C_2 \\ -B_1 \left(I - D_{21}^* R_2^{-1} D_{21}\right) B_1^* & -\left(A - B_1 D_{21}^* R_2^{-1} C_2\right) \end{bmatrix} \tag{0.48}$$

Note that $H_2, J_2 \in \mathrm{dom}(\mathrm{Ric})$ and $X_2 := \mathrm{Ric}(H_2) \geq 0,\ Y_2 := \mathrm{Ric}(J_2) \geq 0$. Let us introduce the concepts of stabilizability and detectability. These are weaker versions of controllability and observability: they only require that the unstable modes be controllable and observable.

Definition: The pair (A, B) is said to be *stabilizable* if there exists a state feedback gain matrix K such that $A + BK$ is stable (all eigenvalues have a negative real part).

Definition: The pair (A, C) is said to be *detectable* if there exists an observer gain matrix L such that $A + LC$ is stable.

Theorem: $\mathcal{H}_2$-Optimal Controller

If the following assumptions hold:

1. *The pair (A, B_2) is stabilizable and the pair (A, C_2) is detectable*
2. $R_1 = D_{12}^* D_{12} > 0$ *(meaning that all of its eigenvalues are positive) and* $R_2 = D_{21}^* D_{21} > 0$
3. $\begin{bmatrix} A - j\omega I & B_2 \\ C_1 & D_{12} \end{bmatrix}$ *has full column rank for all* ω
4. $\begin{bmatrix} A - j\omega I & B_1 \\ C_2 & D_{21} \end{bmatrix}$ *has full row rank for all* ω

Then, the unique $\mathcal{H}_2$-optimal controller minimizing $\|T_{zw}\|_2$ is given by

$$K_{opt}(s) = \left[\begin{array}{c|c} \hat{A}_2 & -L_2 \\ \hline F_2 & 0 \end{array}\right], \qquad (0.49)$$

where matrix L_2 is given by $L_2 := -\left(Y_2 C_2^* + B_1 D_{21}^*\right) R_2^{-1}$, matrix F_2 is given by $F_2 := -R_1^{-1}\left(B_2^* X_2 + D_{12}^* C_1\right)$, and $\hat{A}_2 := A + B_2 F_2 + L_2 C_2$.

Remarks:

- Solutions $X_2 := \mathrm{Ric}(H_2),\ Y_2 := \mathrm{Ric}(J_2)$ of the Riccati equations can be obtained using the Matlab command "lqr".
- The Matlab command "h2syn" directly computes an $\mathcal{H}_2$-optimal controller given the generalized plant model $P(s)$
- Assumptions 3 and 4 ensure that $H_2,\ J_2 \in \mathrm{dom}(\mathrm{Ric})$
- The assumptions usually hold when the problem is well posed. For example, there should always be biproper weighting functions on the control signals, otherwise the optimal controller would produce infinite control signals. This corresponds to matrix D_{12} having full column rank. Likewise, there should be an output disturbance or a measurement noise defined that couples right into the measured signal used by the controller. This corresponds to matrix D_{21} having full column rank.

Example: $\mathcal{H}_2$ design for the mixing tank process

The LTI state-space equations for the mixing tank are

$$\begin{aligned} \frac{d\Delta x(t)}{dt} &= \underbrace{\begin{bmatrix} 0 & 0 \\ 0.0298 & -0.001 \end{bmatrix}}_{A} \Delta x(t) + \underbrace{\begin{bmatrix} 1 & 0 \\ -30 & 2.388\times 10^{-7} \end{bmatrix}}_{B} \Delta u(t) \\ \Delta y(t) &= \underbrace{\begin{bmatrix} 0 & 1 \end{bmatrix}}_{C} \Delta x(t) + d_0(t) \end{aligned} \qquad (0.50)$$

Recall that the states and inputs are $\Delta x_1 = \Delta V\,[m^3]$ and $\Delta x_2 = \Delta T\,[K]$, and $\Delta u_1 = \Delta q_{in}\,[m^3/s]$ and $\Delta u_2 = \Delta Q\,[W]$. We have already checked that (A, B) is controllable and (A, C) is observable. The plant transfer matrix is given by

$$
\begin{aligned}
G(s) &= \begin{bmatrix} \Delta\hat{q}_{in}(s) \\ \Delta\hat{Q}(s) \end{bmatrix} \mapsto \Delta\hat{T}(s) = \left[\begin{array}{c|c} A & B \\ \hline C & 0 \end{array}\right] \\
&= C\left[sI - A\right]^{-1} B \\
&= \begin{bmatrix} 0 & 1 \end{bmatrix} \begin{bmatrix} s & 0 \\ -0.0298 & s+0.001 \end{bmatrix}^{-1} \begin{bmatrix} 1 & 0 \\ -30 & 2.388\times10^{-7} \end{bmatrix} \\
&= \frac{1}{s(s+0.001)} \begin{bmatrix} 0 & 1 \end{bmatrix} \begin{bmatrix} s+0.001 & 0 \\ 0.0298 & s \end{bmatrix} \begin{bmatrix} 1 & 0 \\ -30 & 2.388\times10^{-7} \end{bmatrix}. \\
&= \begin{bmatrix} \dfrac{-30s+0.0298}{s(s+0.001)} & \dfrac{2.388\times10^{-7}}{(s+0.001)} \end{bmatrix} \\
&= \begin{bmatrix} \dfrac{29.8(-1007s+1)}{s(1000s+1)} & \dfrac{2.388\times10^{-4}}{(1000s+1)} \end{bmatrix}
\end{aligned}
\tag{0.51}
$$

Assume that the energy-density spectrum (frequency contents) of the output disturbance is mostly concentrated below 0.001 radians/s, and is modeled by the biproper weighting function

$$
W_o(s) = \frac{0.01s+10}{2000s+1}. \tag{0.52}
$$

The biproper weighting function $W_u(s) = \begin{bmatrix} 10 & 0 \\ 0 & 0.0001 \end{bmatrix}$ is used to constrain the valve and heater responses, while $W_e(s) = \dfrac{10}{2000s+1}$ is used to further reduce the sensitivity at low frequencies.

The generalized plant transfer matrix $P(s) := \begin{bmatrix} P_{11}(s) & P_{12}(s) \\ P_{21}(s) & P_{22}(s) \end{bmatrix}$, is obtained from (0.43):

$$P_{11}(s) = 0$$

$$P_{12}(s) = \begin{bmatrix} W_u \\ W_e G \end{bmatrix} = \begin{bmatrix} \begin{bmatrix} 10 & 0 \\ 0 & 0.0001 \end{bmatrix} \\ \dfrac{10}{(2000s+1)} \begin{bmatrix} \dfrac{29.8(-1007s+1)}{s(1000s+1)} & \dfrac{2.388\times 10^{-4}}{(1000s+1)} \end{bmatrix} \end{bmatrix}$$

$$= \begin{bmatrix} 10 & 0 \\ 0 & 0.0001 \\ \dfrac{298(-1007s+1)}{s(2000s+1)(1000s+1)} & \dfrac{2.388\times 10^{-3}}{(2000s+1)(1000s+1)} \end{bmatrix} \tag{0.53}$$

$$P_{21}(s) = W_o = \frac{10}{2000s+1}$$

$$P_{22}(s) = -G = \begin{bmatrix} \dfrac{-29.8(-1007s+1)}{s(1000s+1)} & \dfrac{-2.388\times 10^{-4}}{(1000s+1)} \end{bmatrix}$$

Using the Matlab m-file *H2mixing.m*, we obtain the fourth-order, proper $\mathcal{H}_2$-optimal controller that yields $\|T_{zw}\|_2 = 1.097$.

2.3 IMC H_2-optimal LTI controller

The internal model control (IMC) approach of Morari is well-suited for $\mathcal{H}_2$-optimization. Recall that an IMC structure uses a nominal internal model of the process and the IMC filter (controller) acts on measured output errors between the process and its model. A block diagram of an IMC structure is shown below.

This is the so-called internal model control (IMC) configuration of Morari and Zafiriou (1989) shown below. The key assumption here is that the plant, the actuators and the sensors are stable, so that all the poles of $G(s), G_a(s), G_m(s)$ are in the open left half-plane. Note that the controller is the feedback interconnection of the extended plant model and the stable IMC controller $Q(s)$. Recall that internal stability of the feedback system is obtained if and only if $Q(s)$ is stable.

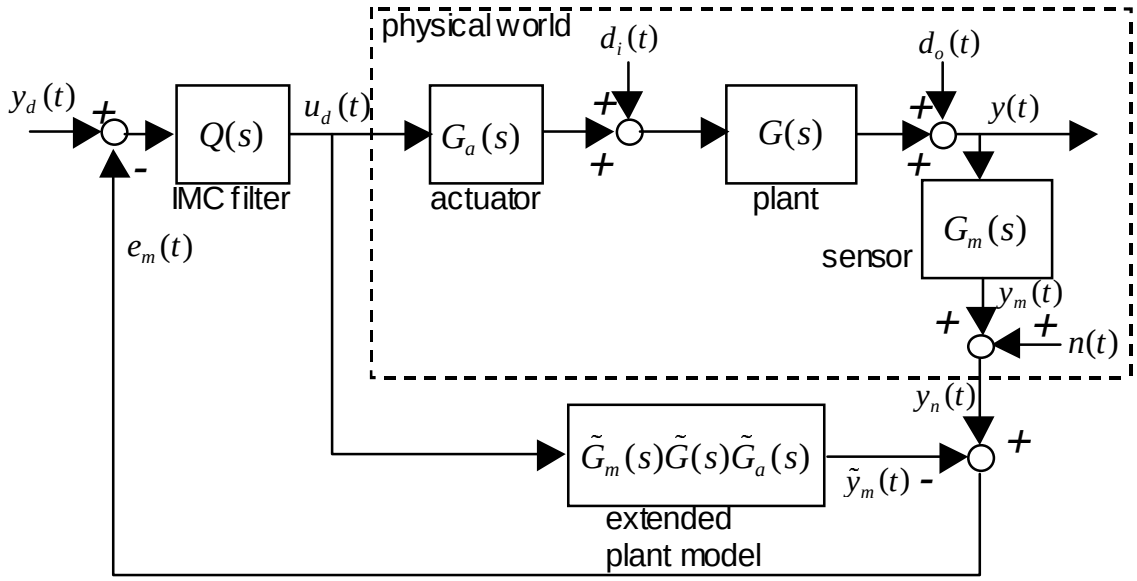

Figure 4: General IMC configuration

The basic idea behind IMC is the following. Suppose that the transfer matrix models for our plant, actuators and sensors are perfect, i.e., $\tilde{G}_m(s) = G_m(s), \tilde{G}(s) = G(s), \tilde{G}_a(s) = G_a(s)$. Also assume that there are no disturbance or noise in the process for now. Then, since the control signal $u_c(t)$ is applied to both the extended plant and its model, we have

$$\hat{e}_m(s) = \hat{y}_n(s) - \hat{\tilde{y}}_n(s) = \left[G_m(s)G(s)G_a(s) - \tilde{G}_m(s)\tilde{G}(s)\tilde{G}_a(s)\right]\hat{u}_c(s) = 0 \qquad (0.54)$$

and therefore there is no internal feedback in the controller that would result from a deviation from the actual measured output of the plant $\tilde{y}_n(t)$ from the desired measured output $y_n(t)$. Hence, both the extended plant and its model operate in open-loop. Now a basic requirement for the IMC filter $Q(s)$ is that it must be stable. Thus, the response of the plant will be the open-loop response of the stable cascade interconnection of $Q(s)$ and $G_m(s)G(s)G_a(s)$:

$$\hat{y}_n(s) = G_m(s)G(s)G_a(s)Q(s)\hat{y}_d(s)\,. \qquad (0.55)$$

From this equation, it is now clear what the ideal IMC controller should be, that is $Q(s) = \left[G_m(s)G(s)G_a(s)\right]^{-1}$ so that we get perfect tracking $\hat{y}_n(s) = \hat{y}_d(s)$. This is the concept of *perfect control* in the IMC literature. However, it is not possible to use such a controller (we don't get anything for free!) because it leads to infinite control signals as we now show. The classical controller $K(s)$ corresponding to this $Q(s)$ can be found by computing the transfer matrix $e_m \mapsto u_d$ in the equivalent block diagram shown below.

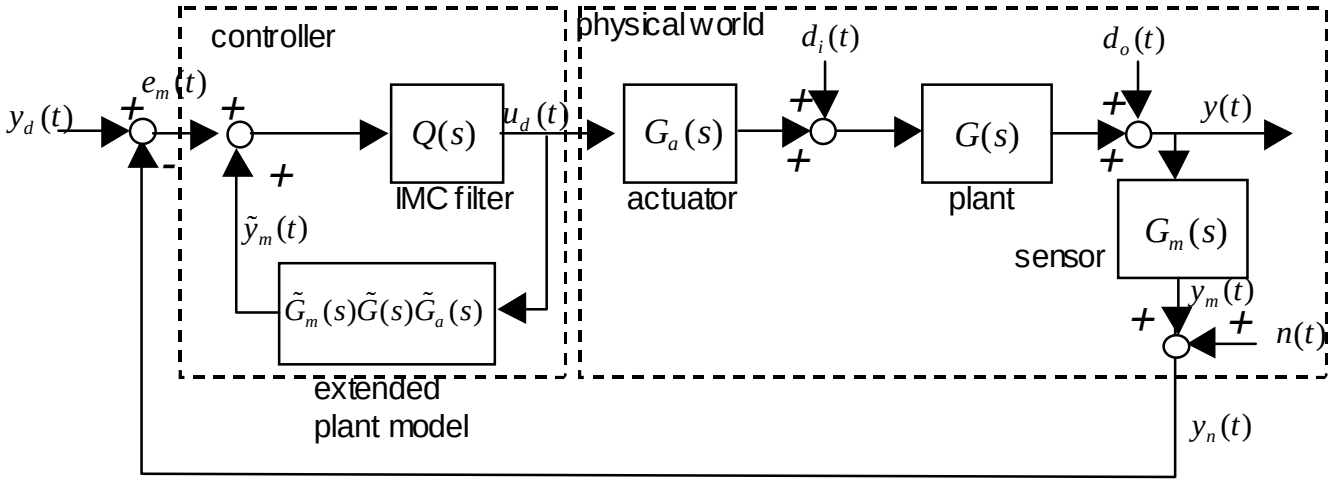

• Figure 5: Block diagram equivalent to IMC configuration

We can see that $K(s)$ is given by the feedback interconnection of $Q(s)$ and the extended plant model $\tilde{G}_m(s)\tilde{G}(s)\tilde{G}_a(s)$:

$$\begin{aligned}\hat{u}_d(s) &= Q(s)\hat{e}_m(s) + Q(s)\tilde{G}_m(s)\tilde{G}(s)\tilde{G}_a(s)\hat{u}_d(s)\\ \hat{u}_d(s) &= \left[I - Q(s)\tilde{G}_m(s)\tilde{G}(s)\tilde{G}_a(s)\right]^{-1} Q(s)\hat{e}_m(s)\end{aligned}. \tag{0.56}$$

Thus,

$$K(s) = \left[I - Q(s)\tilde{G}_m(s)\tilde{G}(s)\tilde{G}_a(s)\right]^{-1} Q(s) \tag{0.57}$$

and for the "perfect" IMC filter, we obtain an infinite controller gain.

$$\begin{aligned}K(s) &= \left[I - \left[\tilde{G}_m(s)\tilde{G}(s)\tilde{G}_a(s)\right]^{-1}\tilde{G}_m(s)\tilde{G}(s)\tilde{G}_a(s)\right]^{-1}\left[\tilde{G}_m(s)\tilde{G}(s)\tilde{G}_a(s)\right]^{-1}\\ &= \infty\end{aligned} \tag{0.58}$$

Even though perfect control is impossible to implement in practice, the concept is important as it provides an ideal scenario to approach in an actual controller design. So the controller design problem using IMC consists of finding a good stable IMC filter such that it approaches perfect control while satisfying all other constraints such as actuator and sensor saturation limits, etc.

Benefits of using an IMC configuration not only for design but also in the actual implementation include:

- It is intuitive,
- There is an internal representation in the controller of what the output signal of the plant should be. This information could be presented to the process operator as a target signal,

- Actuator nonlinearities such as saturation can be included in the internal model such that the control signal generated by the controller takes it into account,
- The IMC filter can be tuned on-line to improve closed-loop performance or robustness.
- Plant delays can be included in the internal model. The controller is then called a *Smith Predictor*.

IMC for unstable plants is the subject of on-going research.

Let's now simplify the IMC block diagram by lumping the plant, the actuators, and the sensors together in $G(s)$. We obtain:

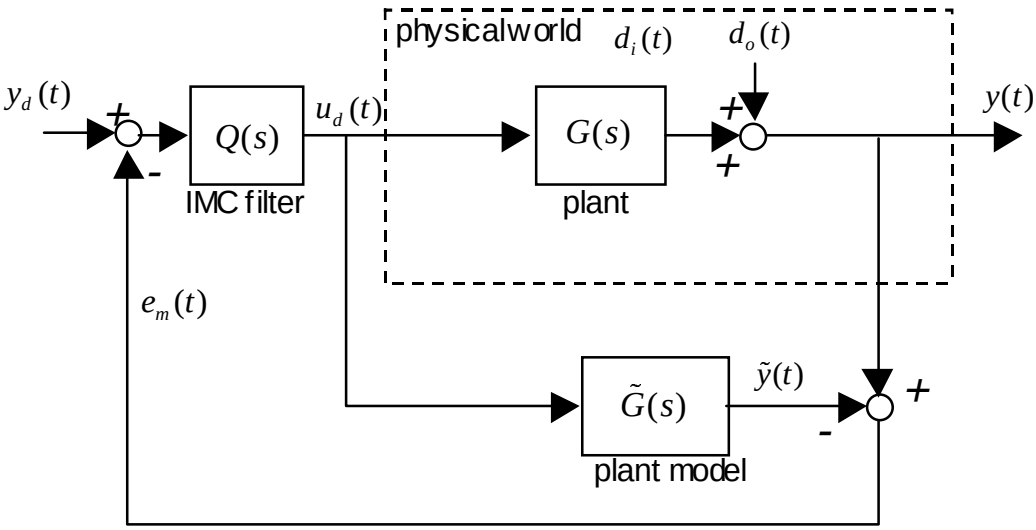

• Figure 6: General IMC configuration

Assuming that there is no uncertainty in the plant model, i.e., $\tilde{G}(s) = G(s)$, both the plant and its model operate in open loop. Recall that $Q(s)$ must be stable to obtain stability in closed-loop. Thus, the response of the plant will be the open-loop response of the stable cascade interconnection of $Q(s)$ and $G(s)$:

$$\hat{y}(s) = G(s)Q(s)\hat{y}_d(s). \tag{0.59}$$

From this equation, the closed-loop transfer matrix from the desired output (the reference) to the actual output (tracking) is given by

$$T_{yy_d}(s) = G(s)Q(s), \tag{0.60}$$

We want to minimize the $\mathcal{H}_2$-norm of the output sensitivity, i.e., the transfer matrix from the output disturbance to the process output: $T_{yd_o}(s) = \hat{d}_o \mapsto \hat{y}$. Let's assume for now that $\tilde{G}(s) \neq G(s)$. The loop equations are solved by solving for u_d first:

$$\begin{aligned} \hat{u}_d &= Q\tilde{G}\hat{u}_d - Q\hat{y} + Q\hat{y}_d \\ \hat{u}_d &= \left(I - Q\tilde{G}\right)^{-1} Q\hat{y}_d - \left(I - Q\tilde{G}\right)^{-1} Q\hat{y} \end{aligned} . \tag{0.61}$$

The output signal is given by:

$$\hat{y} = G\hat{u}_d + \hat{d}_o . \tag{0.62}$$

Substituting this expression in (0.61), we obtain:

$$\begin{aligned} &\hat{y} = G\left(I - Q\tilde{G}\right)^{-1} Q\hat{y}_d - G\left(I - Q\tilde{G}\right)^{-1} Q\hat{y} + \hat{d}_o \\ &\left[I + G\left(I - Q\tilde{G}\right)^{-1} Q\right]\hat{y} = G\left(I - Q\tilde{G}\right)^{-1} Q\hat{y}_d + \hat{d}_o \\ &\Rightarrow \\ &\hat{y} = \left[I + G\left(I - Q\tilde{G}\right)^{-1} Q\right]^{-1} G\left(I - Q\tilde{G}\right)^{-1} Q\hat{y}_d + \left[I + G\left(I - Q\tilde{G}\right)^{-1} Q\right]^{-1} \hat{d}_o \end{aligned} . \tag{0.63}$$

Therefore,

$$T_{yd_o} = \left[I + G\left(I - Q\tilde{G}\right)^{-1} Q\right]^{-1} . \tag{0.64}$$

Finally, assuming perfect modeling $\tilde{G}(s) = G(s)$, we get

$$\begin{aligned} T_{yd_o} &= \left[I + G\left(I - QG\right)^{-1} Q\right]^{-1} \\ &= \left[I + \left(I - GQ\right)^{-1} GQ\right]^{-1} \quad \text{(by the "passing through principle": } \left(I - GQ\right)^{-1} G = G\left(I - QG\right)^{-1}\text{)} \\ &= \left[\left(I - GQ\right)^{-1} (I - GQ + GQ)\right]^{-1} \\ &= I - GQ \end{aligned} \tag{0.65}$$

Note that $T_{yd_o} + T_{yy_d} = I$, which is just the sum of the sensitivity function and the complementary sensitivity function that we denoted as $S + T = I$ in the introductory course.

We wish to find $Q(s) \in \mathcal{RH}_\infty$ such that the $\mathcal{H}_2$-norm $\left\| T_{yd_o} \right\|_2$ is minimized, and the minimization problem can be formulated as:

$$\min_{Q \in \mathcal{RH}_\infty} \left\| (I - GQ)W \right\|_2 . \tag{0.66}$$

where $W(s)$ is a biproper, minimum-phase, stable weighting function that emphasizes frequency bands (usually low frequencies) where the output sensitivity should be small.

2.3.1 Minimum-phase plants

Suppose that the stable $G(s)$ is real-rational and minimum-phase, i.e., all of its zeros lie in the open left half-plane. Then, it is awfully tempting to set $Q = G^{-1}$ since this IMC filter would be stable and would reduce the $\mathcal{H}_2$-norm to zero, irrespective of the weighting function. This is the concept of perfect control again. However, it is not possible to use such a controller because, as shown earlier, it leads to infinite control signals. Moreover, if $G(s)$ rolls off at high frequencies, like most processes do, then $Q(j\omega) = G^{-1}(j\omega)$ would tend to infinity as the frequency tends to infinity, which is undesirable because the closed-loop transfer matrix from the output disturbance to the control signal is given by:

$$\begin{aligned} \hat{u}_d &= Q\tilde{G}\hat{u}_d - Q\left(G\hat{u}_d + \hat{d}_o\right) + Q\hat{y}_d \\ \hat{u}_d &= \left(I - Q\tilde{G} + QG\right)^{-1} Q\hat{y}_d - \left(I - Q\tilde{G} + QG\right)^{-1} Q\hat{d}_o \end{aligned} \tag{0.67}$$

which for $\tilde{G}(s) = G(s)$ simplifies to:

$$T_{u_d d_o} = -Q . \tag{0.68}$$

The optimization of (0.66) is not well-posed. One would have to add the norm of the closed-loop matrix from the output disturbance to the control signal in (0.66) to make it well-posed. Nevertheless, Morari and Zafiriou proposed the concept of an IMC filter that is split up between a part that inverts the process, and another part that rolls off at high frequencies (the *tuning filter*) to make sure that the actuators won't respond violently to high-frequency disturbances or measurement noise. Assuming that $G(s)$ is real-rational and minimum-phase, the IMC controller is proposed as

$$Q = G^{-1} Q_f . \tag{0.69}$$

This controller isn't optimal in the sense that it doesn't minimize (0.66) (in fact, it can make the norm infinite!), but Q_f can be chosen such that it is close to the identity at low frequencies where a low sensitivity is important, and that rolls off faster than the process so that $Q = G^{-1} Q_f$ is strictly proper and thus rolls off at high frequencies.

Example (IMC design simple first-order SISO minimum-phase plant)

Consider the process described by its transfer function $G(s) = \dfrac{2}{s+1}$ and assume that the model is perfect. An IMC controller for this process could be chosen as

$$Q = G^{-1}Q_f = \frac{s+1}{2}Q_f = \frac{s+1}{2}\frac{1}{(s+1)^2} = \frac{1}{2(s+1)}. \tag{0.70}$$

Which would yield the output sensitivity

$$T_{yd_o} = 1 - GQ = 1 - \frac{1}{(s+1)^2} = \frac{s(s+2)}{(s+1)^2} \tag{0.71}$$

and the complementary sensitivity

$$T_{yy_d} = GQ = Q_f = \frac{1}{(s+1)^2}. \tag{0.72}$$

We see that the tuning filter Q_f directly specifies the complementary sensitivity function from the reference to the output: $T_{yy_d} = Q_f$. Hence tracking performance is specified by Q_f.

2.3.2 Non-minimum-phase plants

For non-minimum-phase plants (including plants with delays), we can't invert $G(s)$ with $Q(s)$ as this would result in an unstable $Q(s)$, and hence an unstable control system. What we can do is to invert the invertible (minimum-phase) part of $G(s)$. The minimization problem was formulated as:

$$\begin{aligned} &\min_{Q\in\mathcal{RH}_\infty} \left\|(I - GQ)W\right\|_2 \\ &\equiv \min_{Q\in\mathcal{RH}_\infty} \left\|W - G\bar{Q}\right\|_2 \end{aligned}. \tag{0.73}$$

Write $G(s)$ as a product of two transfer matrices, one that's *all-pass* and one that's *minimum-phase*:

$$G(s) = G_{ap}(s)G_{mp}(s). \tag{0.74}$$

The all-pass factor $G_{ap}(s)$ has all the RHP zeros of $G(s)$ and satisfies $G_{ap}^{*}(j\omega)G_{ap}(j\omega) = I$. Let $G_{ap}^{\sim}(s) := G_{ap}^{T}(-s)$. It is easy to show that if $G_{ap}(s) \in \mathcal{H}_2$, then $G_{ap}^{\sim}(s) \in \mathcal{H}_2^{\perp}$. The latter is also all-pass. Then $G_{ap}(s)$ is such that $G_{ap}^{\sim}(s)G_{ap}(s) = I$, hence $G_{ap}^{\sim}(s) = G_{ap}^{-1}(s)$. We have

$$\left\|W - G\bar{Q}\right\|_2 = \left\|W - G_{ap}G_{mp}\bar{Q}\right\|_2. \tag{0.75}$$

It can be shown that the $\mathcal{H}_2$-norm of a transfer matrix is invariant under multiplication by an all-pass function, thus

$$
\begin{aligned}
\left\|W - G\bar{Q}\right\|_2^2 &= \left\|W - G_{ap}G_{mp}\bar{Q}\right\|_2^2 \\
&= \| \underbrace{G_{ap}^{\sim}W}_{\in \mathcal{H}_2^{\perp}\oplus\mathcal{H}_2} - \underbrace{G_{mp}\bar{Q}}_{\in \mathcal{H}_2} \|_2^2 \\
&= \| \underbrace{\left\{G_{ap}^{\sim}W\right\}_{\mathcal{H}_2^{\perp}}}_{\in \mathcal{H}_2^{\perp}} + \underbrace{\left\{G_{ap}^{\sim}W\right\}_{\mathcal{H}_2} - G_{mp}\bar{Q}}_{\in \mathcal{H}_2} \|_2^2 \\
&= \left\|\left\{G_{ap}^{\sim}W\right\}_{\mathcal{H}_2^{\perp}}\right\|_2^2 + \left\|\left\{G_{ap}^{\sim}W\right\}_{\mathcal{H}_2} - G_{mp}\bar{Q}\right\|_2^2
\end{aligned}
\quad . \tag{0.76}
$$

where $\left\{G_{ap}^{\sim}W\right\}_{\mathcal{H}_2}$ means taking the stable terms (with LHP poles) in the partial fraction expansion of $G_{ap}^{\sim}W$, and $\left\{G_{ap}^{\sim}W\right\}_{\mathcal{H}_2^{\perp}}$ means taking the unstable terms (with RHP poles) in the partial fraction expansion of $G_{ap}^{\sim}W$

Clearly from (0.76), the optimal normalized IMC controller is given by $\bar{Q} = G_{mp}^{-1}\left\{G_{ap}^{\sim}W\right\}_{\mathcal{H}_2}$, and the actual IMC controller is $Q = G_{mp}^{-1}\left\{G_{ap}^{\sim}W\right\}_{\mathcal{H}_2} W^{-1}$. Then the sensitivity and complementary sensitivity functions are:

$$
\begin{aligned}
T_{yd_o} &= I - GQ = I - GG_{mp}^{-1}\left\{G_{ap}^{\sim}W\right\}_{\mathrm{H}_2} W^{-1} = I - G_{ap}\left\{G_{ap}^{\sim}W\right\}_{\mathrm{H}_2} W^{-1} \\
T_{yy_d} &= GQ = GG_{mp}^{-1}\left\{G_{ap}^{\sim}W\right\}_{\mathrm{H}_2} W^{-1} = G_{ap}\left\{G_{ap}^{\sim}W\right\}_{\mathrm{H}_2} W^{-1}
\end{aligned}
\quad . \tag{0.77}
$$

Example: SISO $\mathcal{H}_2$-optimal IMC design

Consider the nonminimum-phase process model

$$
G(s) = \frac{29.8(-1007s+1)}{(500s+1)(1000s+1)} \, . \tag{0.78}
$$

We wish to design an $\mathcal{H}_2$-optimal IMC controller for this process. The transfer function is factorized as a product of an allpass transfer function and a minimum-phase transfer function:

$$
G(s) = \underbrace{\frac{(-1007s+1)}{(1007s+1)}}_{G_{ap}(s)} \underbrace{\frac{29.8(1007s+1)}{(500s+1)(1000s+1)}}_{G_{mp}(s)} \tag{0.79}
$$

with the weighting function representing the spectral contents of the output disturbance

$$
W(s) = \frac{100}{2000s+1} \, . \tag{0.80}
$$

The optimal IMC controller is given by $Q = G_{mp}^{-1}\left\{\tilde{G}_{ap}W\right\}_{\mathcal{H}_2} W^{-1}$. We need to compute $\left\{\tilde{G}_{ap}W\right\}_{\mathrm{H}_2}$ first using a partial fraction expansion:

$$\begin{aligned} \tilde{G}_{ap}(s)W(s) &= \frac{100(1007s+1)}{(-1007s+1)(2000s+1)} \\ &= \frac{-0.0665}{s-1/1007} + \frac{0.0165}{s+1/2000} \end{aligned} \tag{0.81}$$

Thus, $\left\{\tilde{G}_{ap}W\right\}_{\mathcal{H}_2} = \dfrac{0.0165}{s+1/2000}$, the stable part. Finally, the optimal IMC controller is computed to be

$$\begin{aligned} Q &= G_{mp}^{-1}\left\{\tilde{G}_{ap}W\right\}_{\mathrm{H}_2} W^{-1} \\ &= \frac{(500s+1)(1000s+1)}{29.8(1007s+1)}\left(\frac{0.0165}{s+1/2000}\right)\left(\frac{2000s+1}{100}\right) \\ &= 0.0111\frac{(500s+1)(1000s+1)}{(1007s+1)} \end{aligned} \tag{0.82}$$

Notice that this optimal IMC controller isn't proper, so it is appropriate to add a high-frequency pole $Q_f(s) := \dfrac{1}{0.001s+1}$ which will not disturb $Q(s)$ at frequencies of interest:

$$Q = 0.0111\frac{(500s+1)(1000s+1)}{(1007s+1)(0.001s+1)} \tag{0.83}$$

The sensitivity and complementary sensitivity functions are then given by:

$$\begin{aligned} T_{yd_o} &= 1 - GQ = 1 - GG_{mp}^{-1}\left\{\tilde{G}_{ap}W\right\}_{\mathcal{H}_2} W^{-1}Q_f \\ &= 1 - G_{ap}\left\{\tilde{G}_{ap}W\right\}_{\mathcal{H}_2} W^{-1}Q_f \\ &= 1 - \frac{(-1007s+1)}{(1007s+1)}\left(\frac{0.0165}{s+1/2000}\right)\left(\frac{2000s+1}{100(0.001s+1)}\right) \\ &= 1 - 0.33\frac{(-1007s+1)}{(1007s+1)(0.001s+1)} = \frac{1.007s^2 + 1339.3s + 0.67}{(1007s+1)(0.001s+1)} \\ T_{yy_d} &= GQ = 1 - T_{yd_o} = 0.33\frac{(-1007s+1)}{(1007s+1)(0.001s+1)} \end{aligned} \tag{0.84}$$

A Bode plot of the sensitivity if shown below.

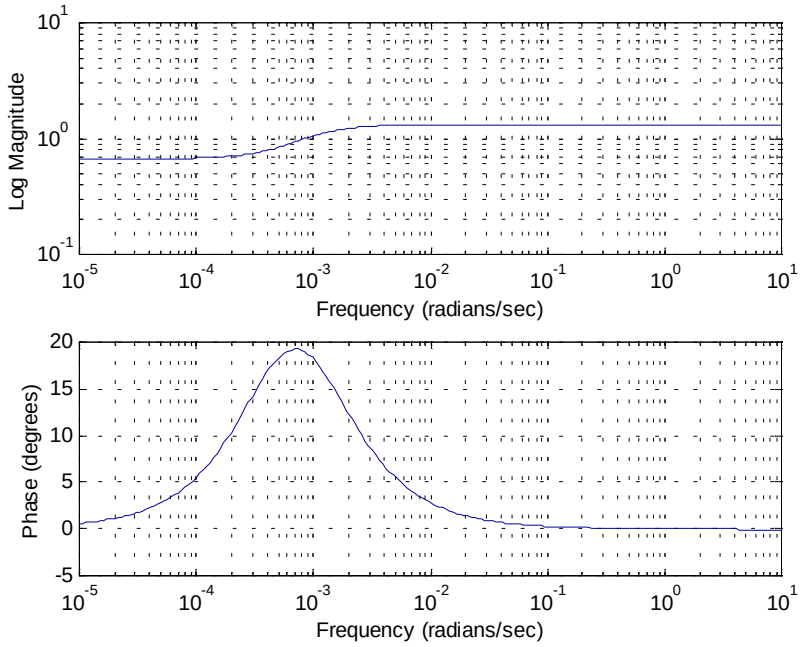

The closed-loop response to an output step disturbance is shown below.

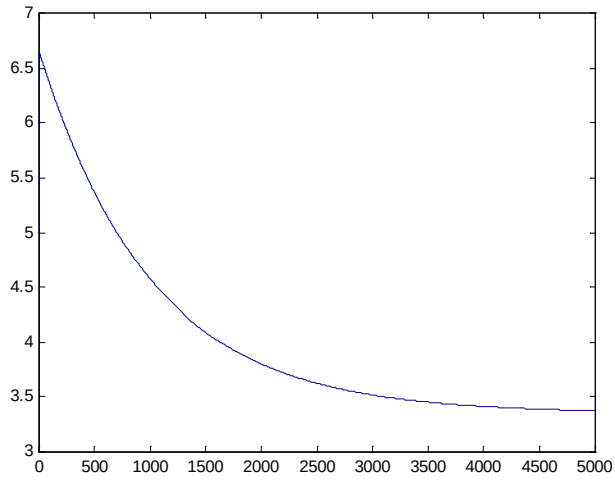

3 H_∞ Optimal Control

$\mathcal{H}_\infty$ optimal control is a theory to design finite-dimensional stabilizing LTI controllers that minimize the $\mathcal{H}_\infty$ -norm of the closed-loop system.

3.1 Problem setup

Consider the block diagram of a feedback control system shown below.

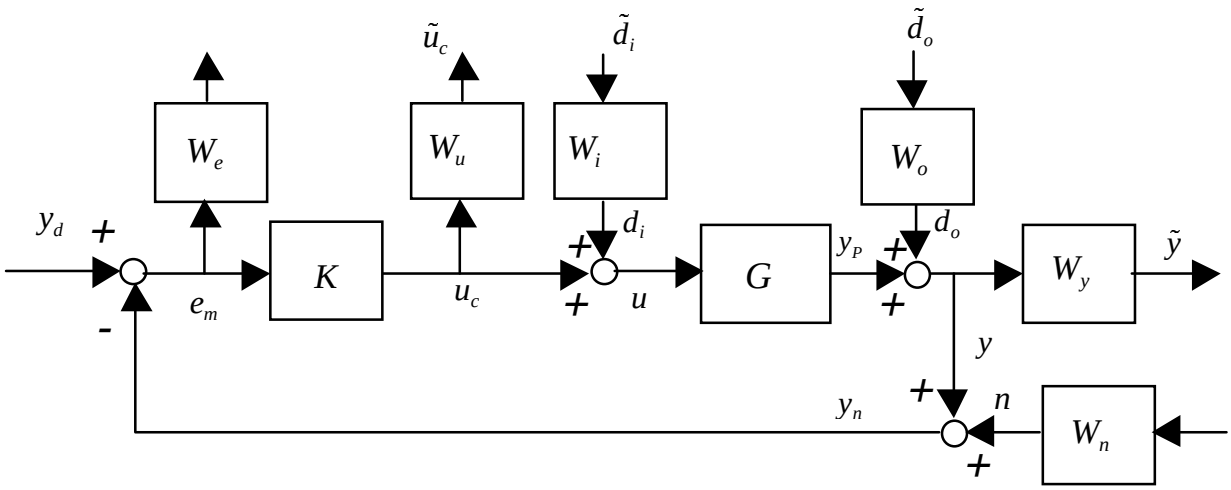

Figure 7: Typical feedback control system

Again, an important step in the $\mathcal{H}_\infty$ controller design process is to select reasonable weighting functions W_d, W_e, W_y, W_u. These weighting functions have a clearer meaning as design parameters than they do in $\mathcal{H}_2$ control because of the definition of the $\mathcal{H}_\infty$ norm of a system. For instance, if the $\mathcal{H}_\infty$ norm of a weighted closed-loop transfer matrix is less than some positive real number γ, i.e., if $\|W(s)T_{zw}(s)\|_\infty < \gamma$, where $W(s)$ is a scalar transfer function, then we have the bound at each frequency $\|T_{zw}(j\omega)\| < \gamma |W^{-1}(j\omega)|$. The weighting function are used to achieve a good tradeoff between concurrent/conflicting closed-loop objectives such as sensitivity minimization and reduction of measurement noise.

For simplicity, we again assume that $\tilde{d}_i = 0, \tilde{n} = 0$, and we consider the regulator problem where the effect of the output disturbance $\tilde{d}_o$ on the weighted output $\tilde{y}$ must be minimized. This system can be recast as a linear fractional transformation (LFT) as follows.

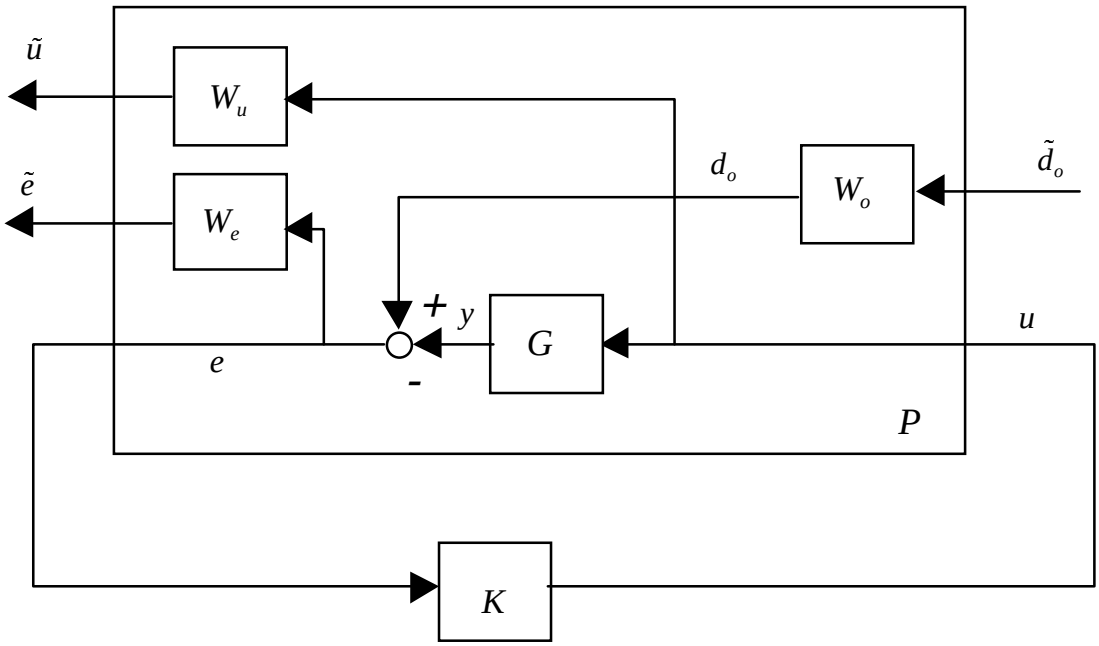

• Figure 8: Typical setup for $\mathcal{H}_\infty$ -optimal control design

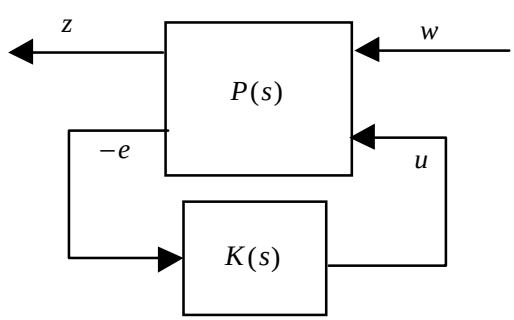

• Figure 9: Standard LFT diagram for $\mathcal{H}_\infty$ -optimal control design

Where $P(s) := \begin{bmatrix} P_{11}(s) & P_{12}(s) \\ P_{21}(s) & P_{22}(s) \end{bmatrix}$, and the transfer matrix entries of this generalized plant were given in (0.43) and are repeated here for convenience:

$$\begin{aligned} P_{11}(s) &= 0 \\ P_{12}(s) &= \begin{bmatrix} W_u \\ W_e G \end{bmatrix} \\ P_{21}(s) &= W_o \\ P_{22}(s) &= -G \end{aligned} \tag{0.85}$$

The weighting function $W_u(s)$ can be used to constrain the control signal at each frequency, while $W_e(s)$ can be used to reduce the sensitivity, typically at low frequencies. Weighting function $W_o(s)$ can be used to model the power spectral density or energy-density spectrum of the output disturbance. Once the control system is put in the form of the so-called standard $\mathcal{H}_\infty$ problem (in LFT form), the minimization problem becomes:

$$\min_{K \in \mathcal{S}} \|T_{zw}\|_\infty \tag{0.86}$$

where $T_{zw}(s) = \mathcal{F}_L[P(s), K(s)]$ is the closed-loop transfer matrix from the exogenous input w to the output z. The optimization of (0.86) is very difficult theoretically and numerically. Virtually everybody uses the solution to the *suboptimal* $\mathcal{H}_\infty$ *problem* stated as

Given $\gamma > 0$ *, find an admissible controller (if there exists any) such that* $\|T_{zw}\|_\infty < \gamma$ *.*

We will present the solution to this problem, and it should be clear that an iterative bisection procedure for reducing γ while checking that a suboptimal controller exists will lead to a controller as close to the optimal controller as desired.

3.2 Solution to simplified suboptimal $\mathcal{H}_\infty$ problem

The solution to the simplified suboptimal $\mathcal{H}_\infty$ problem is obtained from the solutions of a pair of Riccati equations. However, the difference with the $\mathcal{H}_2$ problem is that these Riccati equations cannot be solved independently from one another, making the $\mathcal{H}_\infty$ problem more difficult.

But first, let's discuss the simplifying assumptions that we will use here. The general problem is more involved mathematically, and doesn't provide much more insight. Therefore we will stick with the simplified problem.

Suppose that a state-space realization of the generalized plant $P(s)$ is given by

$$P(s) = \left[\begin{array}{c|cc} A & B_1 & B_2 \\ \hline C_1 & 0 & D_{12} \\ C_2 & D_{21} & 0 \end{array}\right]. \tag{0.87}$$

Notice the special off-diagonal structure assumed for D (just like the $\mathcal{H}_2$ case). Given $\gamma > 0$, define the two Hamiltonian matrices:

$$H_\infty := \begin{bmatrix} A & \gamma^{-2} B_1 B_1^* - B_2 B_2^* \\ -C_1^* C_1 & -A^* \end{bmatrix}, \tag{0.88}$$

$$J_\infty := \begin{bmatrix} A^* & \gamma^{-2} C_1^* C_1 - C_2^* C_2 \\ -B_1 B_1^* & -A \end{bmatrix}. \tag{0.89}$$

Assume that:

1. The pair (A, B_1) is stabilizable and the pair (A, C_1) is detectable,
2. The pair (A, B_2) is stabilizable and the pair (A, C_2) is detectable,
3. $D_{12}^T \begin{bmatrix} C_1 & D_{12} \end{bmatrix} = \begin{bmatrix} 0 & I \end{bmatrix}$ (meaning that the columns of D_{12} are orthonormal, and orthogonal to the columns of C_1)
4. $\begin{bmatrix} B_1 \\ D_{21} \end{bmatrix} D_{21}^T = \begin{bmatrix} 0 \\ I \end{bmatrix}$ (meaning that the rows of D_{21} are orthonormal, and orthogonal to the rows of B_1)

Remarks:

- Assumption 2 is required if we want to stabilize the plant with the controller
- Assumption 1 simplifies the theoretical developments and usually holds in practice
- Assumptions 3 and 4 are also made for technical reasons and practical problems can be set up so that these assumptions hold.

Theorem: $\mathcal{H}_\infty$ Controller

There exists an admissible controller such that $\|T_{zw}\|_\infty < \gamma$ if and only if the following three conditions hold:

1. $H_\infty \in \mathrm{dom}(\mathrm{Ric})$ *and* $X_\infty := \mathrm{Ric}(H_\infty) \geq 0$ *;*

2. $J_\infty \in \mathrm{dom}(\mathrm{Ric})$ *and* $Y_\infty := \mathrm{Ric}(J_\infty) \geq 0$ *;*

3. $\rho\left(X_\infty Y_\infty\right) < \gamma^2$ *(the spectral radius of the product* $X_\infty Y_\infty$ *)*

When these conditions hold, one such controller is

$$K_\infty(s) := \left[\begin{array}{c|c} \hat{A}_\infty & -Z_\infty L_\infty \\ \hline F_\infty & 0 \end{array}\right], \tag{0.90}$$

where

$$\hat{A}_\infty := A + \gamma^{-2} B_1 B_1^* X_\infty + B_2 F_\infty + Z_\infty L_\infty C_2, \tag{0.91}$$

$$F_\infty := -B_2^* X_\infty, \tag{0.92}$$

$$L_\infty := -Y_\infty C_2^*, \tag{0.93}$$

$$Z_\infty := \left(I - \gamma^{-2} Y_\infty X_\infty\right)^{-1}. \tag{0.94}$$

Remarks:

- Solutions $X_\infty := \mathrm{Ric}(H_\infty)$, $Y_\infty := \mathrm{Ric}(J_\infty)$ of the Riccati equations can be obtained using the Matlab command "lqr".

- The theorem suggests an iterative way to find a controller that minimizes the $\mathcal{H}_\infty$-norm of the closed-loop system, based on the bisection idea to compute an $\mathcal{H}_\infty$-norm given earlier. Namely, given a large enough starting value for γ, solve the two Riccati equations and check whether the spectral radius of $X_\infty Y_\infty$ is less than γ^2. Then reduce gamma by half in a bisection scheme, backtracking if needed. Continue the iteration until two consecutive values of gamma representing lower and upper bounds on $\|T_{zw}\|_\infty$ are found to be close enough. Finally, the controller can be computed using the state-space matrices given in (0.90).

- The Matlab command "hinfsyn" directly computes an $\mathcal{H}_\infty$-suboptimal controller given the generalized plant model $P(s)$ and a performance level $\gamma > 0$. It uses the algorithm described above.

Example: $\mathcal{H}_\infty$ design for the mixing tank process

The plant transfer matrix is given by

$$G(s) = \begin{bmatrix} \Delta\hat{q}_{in}(s) \\ \Delta\hat{Q}(s) \end{bmatrix} \mapsto \Delta\hat{T}(s) = \begin{bmatrix} \dfrac{29.8(-1007s+1)}{s(1000s+1)} & \dfrac{2.388\times10^{-4}}{(1000s+1)} \end{bmatrix}. \tag{0.95}$$

Assume that the energy-density spectrum (frequency contents) of the output disturbance is mostly concentrated below 0.001 radians/s, and is modeled by the biproper weighting function

$$W_o(s) = \frac{0.01s+10}{2000s+1}. \tag{0.96}$$

The biproper weighting function $W_u(s) = \begin{bmatrix} 10 & 0 \\ 0 & 0.0001 \end{bmatrix}$ is used to constrain the valve and heater responses, while $W_e(s) = \dfrac{10}{2000s+1}$ is used to further reduce the sensitivity at low frequencies. We also use an input weighting $W_i(s) = 0.001$ to satisfy Assumption 1 ((A, B_1) must be stabilizable.)

The generalized plant transfer matrix $P(s) := \begin{bmatrix} P_{11}(s) & P_{12}(s) \\ P_{21}(s) & P_{22}(s) \end{bmatrix}$, was obtained in (0.43).

Using the Matlab m-file *Hinfmixing.m*, we obtain the following output from hinfsyn (bisection):

```
Test bounds:     0.0000 <  gamma  <=   1000.0000

  gamma    hamx_eig  xinf_eig  hamy_eig   yinf_eig   nrho_xy   p/f
1.000e+003  5.0e-004  2.2e-013  4.0e-004  -4.3e-018    0.0006    p
  500.000  5.0e-004  2.2e-013  4.0e-004  -4.5e-017    0.0023    p
  250.000  5.0e-004  2.2e-013  4.0e-004  -6.8e-018    0.0094    p
  125.000  5.0e-004  2.2e-013  4.0e-004  -1.5e-017    0.0376    p
   62.500  5.0e-004  2.2e-013  4.0e-004  -3.3e-018    0.1505    p
   31.250  5.0e-004  2.2e-013  4.0e-004  -1.9e-017    0.6054    p
   15.625  5.0e-004  2.2e-013  4.0e-004  -2.3e-018    2.4768#   f
   27.057  5.0e-004  2.2e-013  4.0e-004  -8.0e-017    0.8096    p
   24.771  5.0e-004  2.2e-013  4.0e-004  -1.3e-017    0.9678    p
   22.941  5.0e-004  2.2e-013  4.0e-004  -3.8e-017    1.1305#   f
   24.270  5.0e-004  2.2e-013  4.0e-004   7.1e-018    1.0086#   f

 Gamma value achieved:    24.7705
norm between 24.7674 and 24.7921
achieved near 0
```

This indicates that the achieved $\mathcal{H}_\infty$ -norm is $\|T_{zw}\|_\infty = 24.77$. The fourth-order $\mathcal{H}_\infty$ controller in the form $K(s) = \left[\begin{array}{c|c} A & B \\ \hline C & D \end{array}\right]$ displayed below:

```
-8.3e+001  3.2e-017  0.0e+000 -1.2e+003  | -3.1e+005
-8.7e-019 -4.0e-004  0.0e+000  0.0e+000   | -1.7e+001
-1.4e+001 -1.5e-002 -2.1e+001 -2.0e+002  | -5.3e+004
-4.2e+002  4.5e-001  6.2e+002 -6.0e+003  | -1.6e+006
-----------------------------------------------------------|----------
-2.4e-004 -5.7e-005 -7.8e-002 -2.6e-003      |  0.0e+000
-8.6e+001 -2.8e+001 -2.7e+004 -9.1e+002  |  0.0e+000
```

4 Uncertainty Modeling for Robust Control

Any mathematical representation (model) of a physical process needs approximations, which lead to model uncertainties. Different forms of models exist to represent these uncertainties according to what information we want to include in the model. These representations reflect at the same time the knowledge of the physical phenomena that cause these uncertainties and our capacity to represent them in a form that's easy to manipulate.

Consider an aircraft as a physical example, whose parameters vary with the flight conditions (altitude, velocity). Certainly, we can obtain a linear mathematical model for a such system by linearizing the equations of the aircraft at different flight conditions within the flight envelope. This will lead to an interval of variation for each parameter of the model obtained. These intervals of parameter uncertainty may represent structurally and accurately the uncertainties in the model but are not easy to deal with mathematically. On the other hand, we can use a more global representation of the uncertainties as a dynamical perturbation of a nominal transfer matrix.

4.1 Unstructured uncertainty

4.1.1 Additive uncertainty model

Suppose that the unknown transfer matrix $G_p(s)$ of a process differs from a nominal transfer matrix model $G(s)$ that we have of it. We say that $G_p(s)$ is the *perturbed model* and $G(s)$ is the *nominal model.* The difference between these two models comes from an unknown dynamical perturbation $\Delta(s)$ representing the unmodeled dynamics of the process. Suppose that this perturbation is additive, call it $\Delta_a(s)$, and that we know a function $\delta_a(\omega) \geq 0$ that bounds its norm (maximum singular value) for each frequency:

$$G_p(s) = G(s) + \Delta_a(s) \tag{0.97}$$

with

$$\|\Delta_a(j\omega)\| < \delta_a(\omega), \forall \omega . \tag{0.98}$$

Note that the upper bound $\delta_a(\omega)$ represent the "size" of the uncertainty of the model at each frequency. It is often taken to be the magnitude of a scalar transfer function. This form of representation is called *additive uncertainty* because the perturbation's transfer matrix is added to the nominal model. This type of uncertainty is also called *unstructured* because the only information we use is just the upper bound of the norm of the uncertainty, and not its structure. That is, $\Delta_a(s)$ can be any transfer matrix that satisfies (0.98).

The figure below shows a closed loop system with such an additive uncertainty model. Again, it is important to emphasize that *we don't know what* $\Delta_a(s)$ *is, we only know that it is bounded by* $\|\Delta_a(j\omega)\| < \delta_a(\omega), \forall \omega$.

We can define a *family of perturbed plant models* as the set

$$\mathcal{P} := \left\{ G_p(s) : \left\| \Delta_a(j\omega) \right\| < \delta_a(\omega) \right\}. \tag{0.99}$$

Then, robust control theory assumes that the unknown, "true" plant model belongs to $\mathcal{P}$. Thus, robust control design consists of designing a controller that can maintain a desired performance level for all plants in $\mathcal{P}$ (robust performance) or just stabilize all plants in $\mathcal{P}$ (robust stability).

Returning to the aircraft example, we might choose the nominal model $G(s)$ as the transfer matrix corresponding to an average flight condition. We can obtain $\delta_a(\omega)$ by calculating a large, but finite number of perturbed transfer matrices $\left\{ G_{pi}(s) \right\}_{i=1}^{N}$ corresponding to various possible flight conditions (altitudes and Mach numbers). It is then reasonable to expect that the corresponding additive perturbation $\Delta_a(s)$ would be bounded by:

$$\max_{i=1,\ldots,N} \left\| G_{pi}(j\omega) - G(j\omega) \right\| \tag{0.100}$$

at each frequency. We would then try to find an uncertainty bound $\delta_a(\omega)$ such that

$$\max_{i=1,\ldots,N} \left\| G_{pi}(j\omega) - G(j\omega) \right\| < \delta_a(\omega). \tag{0.101}$$

To avoid getting too much uncertainty in the model, the upper bound $\delta_a(\omega)$ should be "tight", i.e., it should be close to the left-hand side of (0.101). This would prevent a subsequent robust controller design to be too conservative, i.e., robust to more uncertainty than warranted by our knowledge of the process, but with poor performance. In other words, putting too much uncertainty in the model may be detrimental to the achievable closed-loop performance level. This is an expression of the well-known robustness/performance tradeoff of feedback control.

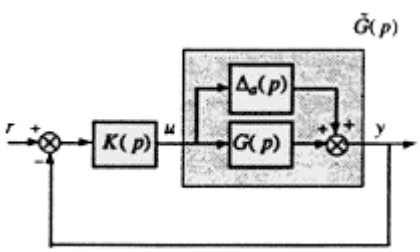

Figure 10: Additive uncertainty

Another way to represent the uncertainty in the system under study is the direct *multiplicative uncertainty* that can be related to additive uncertainty. This uncertainty has two forms of representation:

4.1.2 Output multiplicative uncertainty

The first representation is for direct multiplicative uncertainty taken at the output of the system:

$$G_p(j\omega) = (I_p + \Delta_m(j\omega))G(j\omega) \tag{0.102}$$

with

$$\|\Delta_m(j\omega)\| < \delta_m(\omega) \quad \forall\omega . \tag{0.103}$$

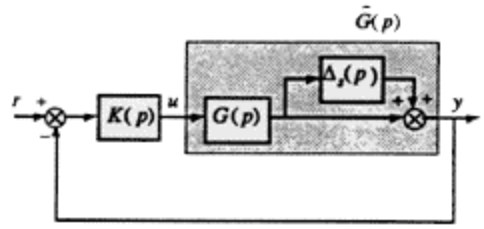

Figure 11: Output multiplicative uncertainty

Example: room heating process with uncertain sensor dynamics

Suppose that the room heating process has a temperature sensor with first-order dynamics that has 10% uncertainty in its frequency response, i.e., $\|\Delta_l(j\omega)\| < 0.1$, $\forall\omega$. This uncertainty can be modeled with an output multiplicative model:

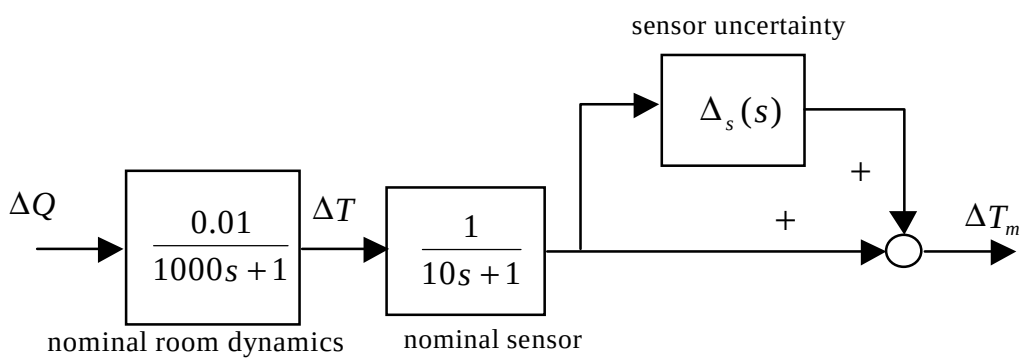

Figure 12: Output multiplicative uncertainty in sensor dynamics

The Nyquist plots of all possible perturbed plant frequency responses produce a Nyquist "band" in the complex plane, as shown in the figure below.

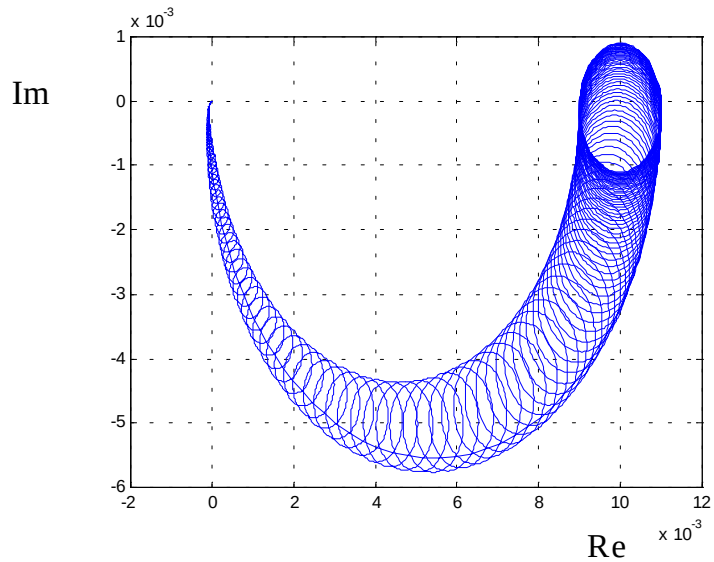

Figure 13: Nyquist band corresponding to output multiplicative uncertainty

4.1.3 Input multiplicative uncertainty

The second perturbed model is such that the direct multiplicative uncertainty appears at the input of the system:

$$G_p(j\omega) = G(j\omega)(I_m + \Delta_m(j\omega)) \tag{0.104}$$

with

$$\|\Delta_m(j\omega)\| < \delta_m(\omega) \quad \forall \omega . \tag{0.105}$$

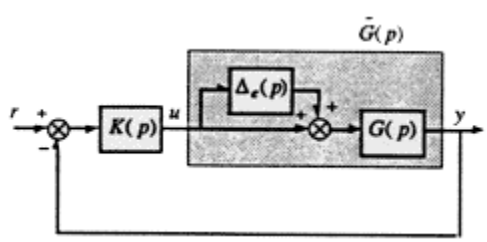

Figure 14: Input multiplicative uncertainty

4.1.4 Input inverse multiplicative uncertainty

The input inverse multiplicative uncertainty can be useful to represent uncertainties that appear in the denominators (e.g., poles) of sensor transfer functions:

$$G_p(j\omega) = (I_p + \Delta_{is}(j\omega))^{-1} G(j\omega) \tag{0.106}$$

with

$$\|\Delta_{is}(j\omega)\| < \delta_{is}(\omega)\,,\ \forall\omega \tag{0.107}$$

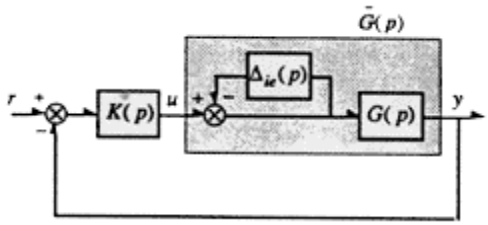

Figure 15: Input inverse multiplicative uncertainty

4.1.5 Output inverse multiplicative uncertainty

The output inverse multiplicative uncertainty may be used to model uncertainties that appear in the denominators (e.g., poles) of actuators transfer functions:

$$G_p(j\omega) = G(j\omega)(I_m + \Delta_i(j\omega))^{-1} \tag{0.108}$$

with

$$\|\Delta_i(j\omega)\| < \delta_i(\omega)\,,\ \forall\omega\,. \tag{0.109}$$

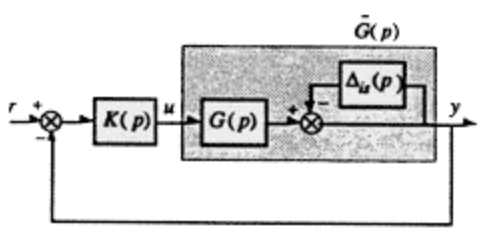

Figure 16: Output inverse multiplicative uncertainty

4.1.6 Feedback uncertainty

The perturbed model is a feedback interconnection of the nominal process model and the perturbation:

$$G_p(j\omega) = G(s)\left[I_m + \Delta_f(s)G(s)\right]^{-1} = \left[I_m + G(s)\Delta_f(s)\right]^{-1} G(s) \tag{0.110}$$

with

$$\left\|\Delta_f(j\omega)\right\| < \delta_f(\omega) \quad \forall\omega\,. \tag{0.111}$$

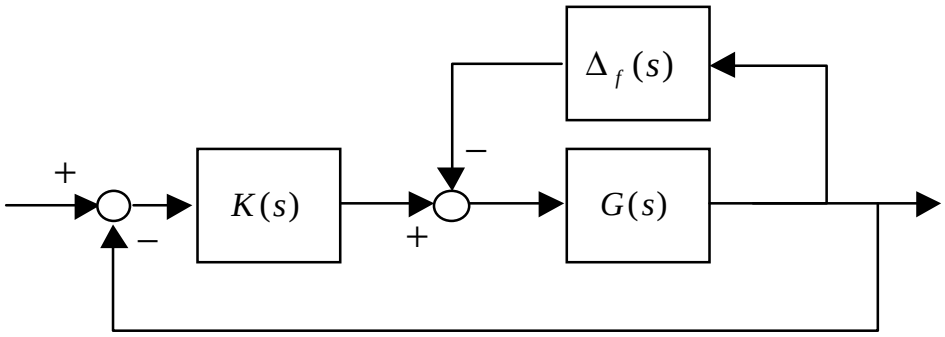

Figure 17: Feedback uncertainty

4.1.7 Linear fractional uncertainty

The perturbed model is a linear fractional transformation (LFT) of the nominal process model on the perturbation:

$$\begin{aligned} G_p(s) &= F_U\left[P(s), \Delta_l(s)\right] = P_{22}(s) + P_{21}(s)\left[I - \Delta_l(s)P_{11}(s)\right]^{-1}\Delta_l(s)P_{12}(s) \\ &= P_{22}(s) + P_{21}(s)\Delta_l(s)\left[I - P_{11}(s)\Delta_l(s)\right]^{-1}P_{12}(s) \end{aligned} \tag{0.112}$$

with

$$\left\|\Delta_l(j\omega)\right\| < \delta_l(\omega)\,, \quad \forall\omega\,. \tag{0.113}$$

The figure below shows a feedback controlled upper LFT with the perturbation.

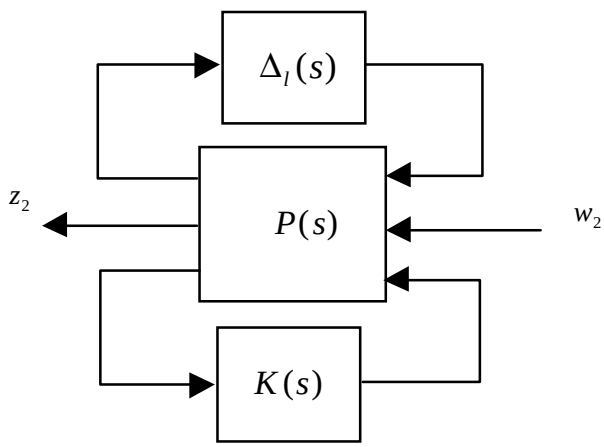

Figure 18: Linear fractional uncertainty

Note that any type of uncertainty described above can be expressed in an LFT form.

Example: Output multiplicative uncertainty expressed in LFT form

Output multiplicative uncertainty can be written as

$$\begin{aligned} G_p(s) &= \left[I_p + \Delta_m(s)\right]G(s) \\ &= G(s) + \Delta_m(s)G(s) \\ &= P_{22}(s) + P_{21}(s)\left[I - \Delta_m(s)P_{11}(s)\right]^{-1}\Delta_m(s)P_{12}(s) \end{aligned} \tag{0.114}$$

and by identification with the entries of $P(s)$, we get

$$P_{22}(s) = G(s), \quad P_{21}(s) = I, \quad P_{11}(s) = 0, \quad P_{12}(s) = G(s) \tag{0.115}$$

For the room heating process with uncertain temperature sensor dynamics:

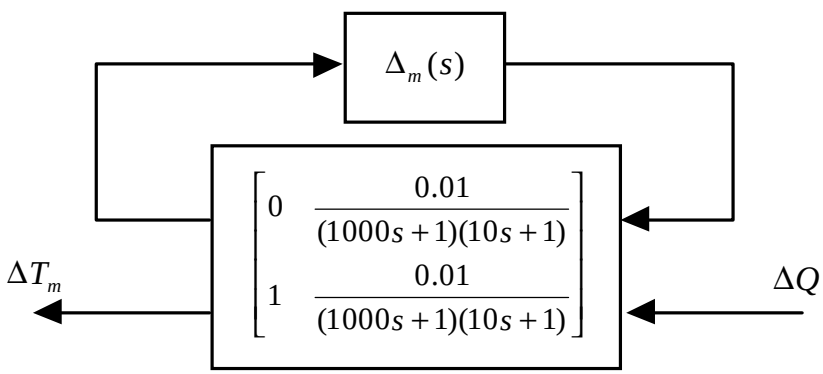

Figure 19: Equivalent linear fractional uncertainty model

Certainly, with such unstructured uncertainty models, we can be conservative and even lose some information about the uncertainty in the physical system, but these kinds of models are general and can represent, lumped into the same model, different uncertainties of different natures. Consider different types on uncertainties and see what perturbation models can represent these uncertainties:

Unmodeled process dynamics at high frequencies: Uncertainty in the roll-off rate of the process model can be represented by multiplicative uncertainty models, or the additive uncertainty model.

Parametric uncertainty: Variation in the model parameters can be represented by the additive uncertainty model, the direct multiplicative model and also the inverse model if the system is square by comparing $G(j\omega)^{-1}$ and $G_p(j\omega)^{-1}$.

Actuator uncertainty: This type of uncertainty essentially comes from the fact that the dynamics of the process actuators may not be well known, or may have been neglected. These uncertainties can be take into account by using the two forms of direct and inverse multiplicative uncertainty at the input.

Sensor uncertainty: Sensors are often sensitive devices that can be partially damaged and deliver slightly erroneous measures. Sensor uncertainty can be represented by the direct and the reverse multiplicative uncertainties at the output.

Nonlinearity and reduction of the model: Non-linearities can be taken into account if their effect can be bounded in the frequency domain (this is not always the case!). Model reduction is often used to simplify the control design. When model reduction techniques are used, we can take into account the neglected dynamics as uncertainty that can be represented by any type of model uncertainty.

4.1.8 Representing uncertainty in the frequency domain

The frequency domain approach, and more specifically the $\mathcal{H}_\infty$ theory, gives the necessary tools to quantify the uncertainties modeled for the physical system under study. Through the example below, we give more details on how the uncertainty regions could be represented by a complex norm-bounded perturbation around a nominal plant.

Suppose we have the perturbed SISO system:

$$G_p(s) = G(s) + W_a(s)\tilde{\Delta}_a(s)\,, \tag{0.116}$$

$$\left|\Delta_a(j\omega)\right| < 1,\ \forall\omega \tag{0.117}$$

where $\tilde{\Delta}_a(s)$ is any *stable* transfer function which, at each frequency, is no larger than one in magnitude (the tilde indicates normalization), and $W_a(s)$ is a *weighting function bounding the uncertainty*. This means that at each frequency, and by considering all $\tilde{\Delta}_a(s)$, $\tilde{\Delta}_a(j\omega)$ generates a disc in the complex plane with radius 1 centered at 0, which implies that $G_p(j\omega)$ generates at each frequency a disk of radius $\left|W_a(j\omega)\right|$ centered at $G(j\omega)$.

For the multiplicative uncertainty case, where the perturbed SISO plant model is

$$G_p(s) = G(s)(I + W_m(s)\tilde{\Delta}_m(s)), \tag{0.118}$$

we can give an analogous description of $G_p(j\omega)$ as given above for which the radius of the disk is $|G(j\omega)W_m(j\omega)|$ rather than $|W_a(j\omega)|$.

The weighting functions used in the perturbed plant can be seen as a normalization of the block uncertainty in order to bound its $\mathcal{H}_\infty$-norm by one. In fact these weighting functions gives the amount of uncertainty that the closed-loop system has to tolerate. The weighting function, for the additive uncertainty, can be obtained by finding the radius:

$$r_a(\omega) := \max_{G_p \in \mathcal{P}} |G_p(j\omega) - G(j\omega)|, \tag{0.119}$$

and then the rational transfer function $W_a(s)$ is found so that:

$$|W_a(j\omega)| \geq r_a(\omega), \forall \omega. \tag{0.120}$$

For the multiplicative case, the radius to find is given by:

$$r_m(\omega) := \max_{G_p \in \mathcal{P}} \left| \frac{G_p(j\omega) - G(j\omega)}{G(j\omega)} \right|. \tag{0.121}$$

For parametric uncertainty we can also derive a complex multiplicative uncertainty block, that allows us to "cover" variations in the process parameters. In order to explain this further, we consider the perturbed system:

$$G_p(s) = \frac{k}{\tau s + 1} e^{-\theta s} \tag{0.122}$$

where $2 \leq k, \theta, \tau \leq 3$.

The objective is to represent this set of models using a multiplicative uncertainty. This facilitates the controller design procedure. In order to reach our objective, we have to use a central model that we considered as a nominal model. One of the methods to do that is to use the mean parameters values and also we can use a low-order model.

In the case of the example we gave before, the nominal model will be a delay-free model: $G(s) = \frac{\bar{k}}{\bar{\tau} s + 1} e^{-\bar{\theta} s} = \frac{2.5}{2.5s + 1}$. To find the multiplicative radius $r_m(\omega) = \max_{G_p} \left| \frac{G_p(j\omega) - G(j\omega)}{G(j\omega)} \right|$ we use the frequency plots $G_p(j\omega)$ for different parameters variation and especially the extreme variations. The rational weight $W_m(j\omega)$ must cover all different plots of r_m such that $W_m(j\omega) \geq r_m(\omega)$.

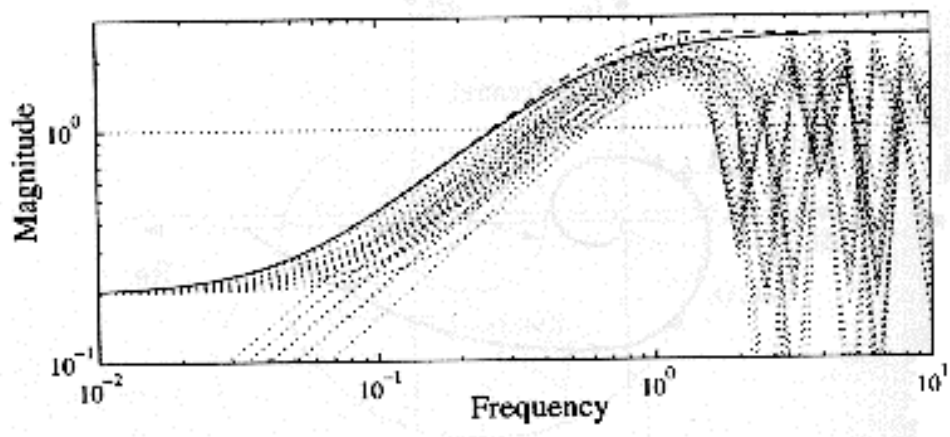

Figure 20: Covering multiplicative uncertainty with a weighting function

The dotted lines are the $r_m(\omega)$. The first weighting function (first try of fitting) is:

$$\frac{Ts+0.2}{(T/2.5)s+1}, T=4 \tag{0.123}$$

It doesn't fit very well. After a gain correction, we got a better weighting function: (The dashed line):

$$\frac{Ts+0.2}{(T/2.5)s+1}\times\frac{s^2+1.6s+1}{s^2+1.4s+1} \tag{0.124}$$

4.2 Theorems for robust closed-loop stability with unstructured uncertainty

We will now discuss the stability of closed-loop systems subject to uncertainties. For each of the different type of the uncertainty described above we will obtain a condition of robust stability that can be exploited.

Two approaches are used to deduce the conditions of the robust stability problem. The first is based on the Nyquist criterion and the second one uses the “small-gain theorem”. Both of the theorems lead to the same robust stability conditions but the required assumptions are not the same.

Let $L(s) := G(s)K(s)$ be the nominal loop gain, and $L_p(s) := G_p(s)K(s)$ the perturbed loop gain, and consider the feedback systems depicted below.

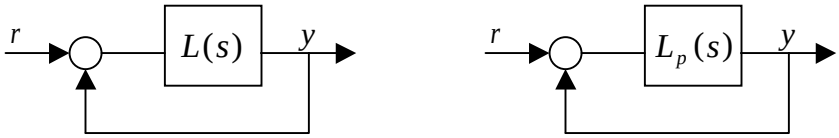

Figure 21: nominal and perturbed closed-loop systems

The following theorem gives a sufficient condition for the stability of the closed-loop perturbed system.

Theorem:

Assume that the following conditions hold:

(A1)- $L(s)$ *and* $L_p(s)$ *have the same number of unstable poles (Re(s)>0).*

(A2)- If $L_p(s)$ *has poles on the imaginary axis, they are also poles of* $L(s)$ *.*

(A3)-The nominal closed-loop system is stable.

Then, the perturbed closed-loop system is stable if for each s *belonging to the Nyquist contour and every* $\varepsilon \in [0,1]$*:* $\det[I + (1-\varepsilon)L(s) + \varepsilon L_p(s)] \neq 0$ *.*

Remarks

- The proof uses the Nyquist band produced by all possible perturbed loop gains.
- This theorem doesn't apply directly to practical robustness problems. Rather, it is used to prove more specific robustness conditions that can be computed using given data (nominal transfer matrices and size of uncertainty)

Another formulation for this theorem can be stated in the following way:

Under the assumptions A1, A2, A3 of the previous theorem, The perturbed system is stable if one of the two following conditions hold:

(C1) $\forall \omega \in \mathbb{R}$, $\bar{\sigma}\left\{[I + L(j\omega)]^{-1}\left[L_p(j\omega) - L(j\omega)\right]\right\} < 1 \Leftrightarrow \left\|(I+L)^{-1}(L_p - L)\right\|_\infty < 1$. (0.125)

(C2) $\forall \omega \in \mathbb{R}$, $\bar{\sigma}\left\{\left[L_p(j\omega) - L(j\omega)\right][I + L(j\omega)]^{-1}\right\} < 1 \Leftrightarrow \left\|(L_p - L)(I+L)^{-1}\right\|_\infty < 1$. (0.126)

For the SISO case these two conditions reduce to a single condition written as:

$$\forall \omega \in \mathbb{R}, \quad \left|G_p(j\omega)K(j\omega) - G(j\omega)K(j\omega)\right| < \left|1 + G(j\omega)K(j\omega)\right| \qquad (0.127)$$

This inequality, in fact, from the figure (), says that the robust stability condition is satisfied if, for each point of the nominal Nyquist plot of $G(j\omega)K(j\omega)$, the circle of center $G(j\omega)K(j\omega)$ and radius $\left|G_p(j\omega)K(j\omega) - G(j\omega)K(j\omega)\right|$ doesn't contain the critical point (-1). This condition is shown in the figure below.

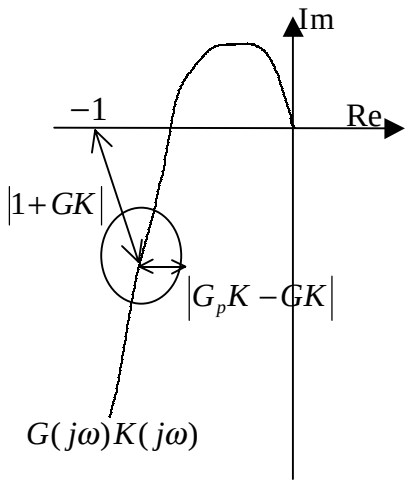

Figure 22: Nyquist plot showing robust stability condition

We now discuss the second approach to the robust stability problem, using the small-gain theorem. Consider in the LFT in the figure below. The matrix $\Delta(s)$ represents the uncertainty in the model and $M(s)$ the nominal matrix transfer function of the closed-loop system. All of the models with different types of uncertainties can be recast in the $M-\Delta$ format. The intermediate step to achieve this is to transform the block diagram into an LFT first as sown below: Then $M(s)=\mathcal{F}_L\left[P(s),K(s)\right]$.

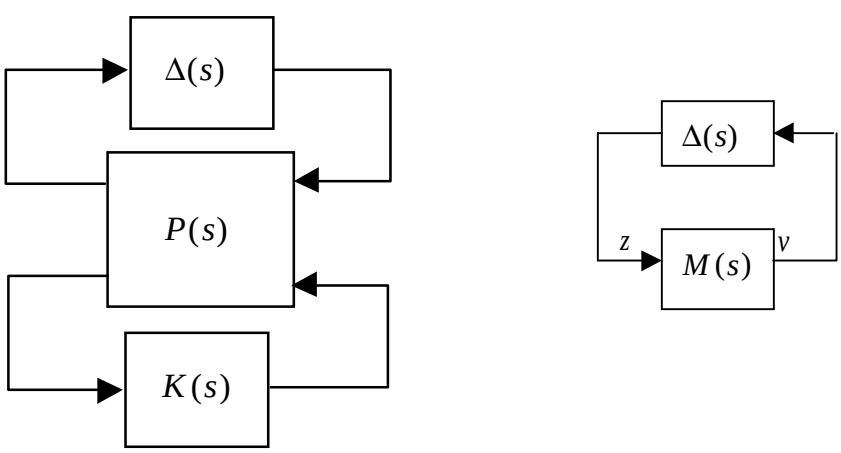

Figure 23: Equivalent LFT and $M-\Delta$ interconnections

Small-Gain Theorem:

Under the assumption (A4) that $M(s)$ *and* $\Delta(s)$ *are stable, i.e.,* $M(s) \in \mathcal{RH}_\infty$, $\Delta(s) \in \mathcal{RH}_\infty$,

the $M - \Delta$ *interconnection shown above is stable for every perturbation* $\Delta(s)$ *such that* $\|\Delta\|_\infty < 1$ *iff* $\|M\|_\infty \leq 1$.

This theorem gives a necessary and sufficient condition for robust stability under the assumptions that the nominal closed-loop system $M(s)$ is stable, and that the uncertainty $\Delta(s)$ is also stable and normalized to have an $\mathcal{H}_\infty$-norm less than 1. The assumption that $\Delta(s)$ be stable is not too restrictive since such perturbations can generate *unstable* perturbed plant models with appropriate uncertainty models, such as inverse multiplicative or feedback uncertainty models.

We apply in the following subsections the robust stability theorems presented above to the various types of uncertainties. For each case we'll deduce a robust stability condition that guarantees the stability of the perturbed closed-loop system.

4.2.1 Robust stability with additive uncertainty

Theorem

Under assumptions (A1), (A2), (A3), the closed-loop system in is stable if:

$$\forall \omega \in \mathbb{R}, \qquad \|\Delta_a(j\omega)\| \left\| K(j\omega)\left[I_p + G(j\omega)K(j\omega)\right]^{-1} \right\| < 1. \tag{0.128}$$

Under assumptions (A4), the closed-loop system in figure() is stable if and only if:

$$\forall \omega \in \mathbb{R}, \qquad \left\| K(j\omega)\left[I_p + G(j\omega)K(j\omega)\right]^{-1} \right\| \leq \delta_a^{-1}(\omega) \tag{0.129}$$

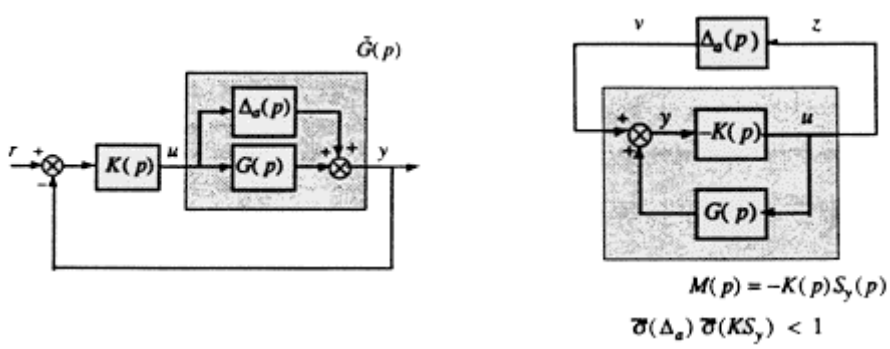

Figure 24: Equivalent $M - \Delta$ interconnection for additive uncertainty

Sketch of Proof: Using the approach based on the Nyquist contour, and under assumptions (A1), (A2), (A3), the nominal and perturbed open loop matrices are given as follows:

$$L(s) = G(s)K(s)\,, \tag{0.130}$$

$$L_p(s) = G_p(s)K(s) = (G(s) + \Delta_a(s))K(s)\,. \tag{0.131}$$

Hence $L_p(s) - L(s) = \Delta_a(s)K(s)$ such that condition (C2) is equivalent to (recall that $\|Q\| = \bar{\sigma}(Q)$):

$$\bar{\sigma}(\Delta_a(j\omega))\bar{\sigma}(K(j\omega)(I_p + G(j\omega)K(j\omega))^{-1}) < 1\,. \tag{0.132}$$

Using the second approach (small-gain theorem), and under the assumption (A4), we have to put the closed loop system in the $M - \Delta$ form. For this we have to isolate the matrix $\Delta(s)$ and calculate the nominal matrix $M(s)$. We obtain $M(s)$ by calculating the transfer matrix between the input z and the output v of $\Delta(s)$. Specifically for the additive case, and in the absence of the reference signal:

$$z = u - Ky = -K(Gz + v) \Leftrightarrow z = -K(I_p + GK)^{-1}v\,. \tag{0.133}$$

This equation correspond in fact to Figure 24. Using

$$M(s) = \mathcal{F}_L\left[P(s), K(s)\right] = -K(s)(I_p + G(s)K(s)) \tag{0.134}$$

and by applying the small-gain theorem, we derive the robust stability condition given above.

Note that both approaches lead to the same robust stability condition, but the assumptions of the first approach are less conservative than in the second approach where $\Delta(s)$ has to be stable.

In fact the robust stability condition for additive uncertainty can be written as :

$\bar{\sigma}(\Delta_a(j\omega))\bar{\sigma}(K(j\omega)S_y(j\omega)) < 1$ where S_y is the output sensitivity. In robust control design, we have to decrease the term $K(j\omega)S_y(j\omega)$ so that the system can tolerate more additive uncertainty.

4.2.2 Robust stability with multiplicative uncertainty

Input multiplicative uncertainty

Theorem

Under assumptions (A1), (A2), (A3), the closed-loop system in the figure below is stable if:

$$\forall \omega \in \mathbb{R}\ ,\ \|\Delta_s(j\omega)\| \left\| K(j\omega)G(j\omega)\left[I_m + K(j\omega)G(j\omega)\right]^{-1} \right\| < 1\ , \qquad (0.135)$$

or, equivalently, $\left\| K(j\omega)G(j\omega)\left[I_m + K(j\omega)G(j\omega)\right]^{-1} \right\| < \delta_m^{-1}(\omega)$. *(0.136)*

Under assumption (A4), the closed-loop system in the figure below is stable if and only if:

$$\forall \omega \in \mathbb{R}\ ,\ \left\| K(j\omega)G(j\omega)\left[I_m + K(j\omega)G(j\omega)\right]^{-1} \right\| < \delta_m^{-1}(\omega)\ . \qquad (0.137)$$

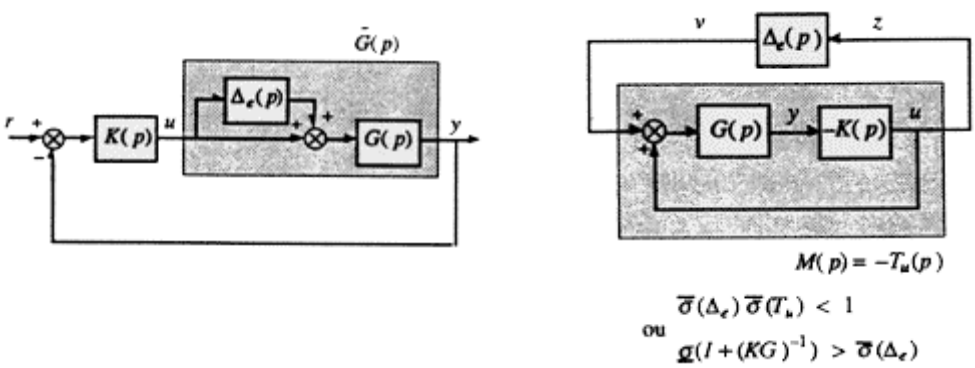

Figure 25: Equivalent $M - \Delta$ interconnection for input multiplicative uncertainty

This last condition can be written as: $\|T_u(j\omega)\| < \delta_m^{-1}(\omega)$, where

$$T_u(s) := K(s)G(s)\left[I_m + K(s)G(s)\right]^{-1} \qquad (0.138)$$

is the input complementary sensitivity matrix. We can see from the robust stability condition for an input multiplicative uncertainty, that T_u reflects the capacity of the system to tolerate uncertainty in the actuators.